NTNU
Norwegian University of
Science and Technology

Physiological Characterization of Protocerebral Neurons in the Olfactory Network of the Moth, *Heliothis virescens*

Nicholas Hagen Kirkerud

Biology
Submission date: July 2011
Supervisor: Hanna Mustaparta, IBI
Co-supervisor: Bjarte Bye Løfaldli, IBI

Norwegian University of Science and Technology
Department of Biology

FORWORD

This study was conducted in the Neuroscience Unit, Department of Biology, under supervision of Professor Hanna Mustaparta and PhD fellow Bjarte Bye Løfaldli. The two past years at the lab have been extraordinary interesting and fun, and I thank all of you whom I have shared this pleasant time with.

I would like to give special thanks to Bjarte, for sharing his highly contagious enthusiasm as well as his practical experience and theoretical knowledge. I will not easily forget our many fruitful discussions, nor the excitement and dissapointment we shared in the lab. I am also very thankful for all data material you have provided, and trusted me with. I would also like to thank Dr. Pål Kvello, for teaching me the essence of Amira and some of its many wonders. Thanks to Dr. Bente Berg, for sharing her philosophical insight, and her impressive collection of comical episodes.

A big thanks to my family, for being supportive and believing in me. A special thanks to Nina Orucevic, her patience throughout the period of my thesis means a lot to me. Thanks for cheering me up, and for always having confidence in me.

Finally, I would like to thank my supervisor, Professor Hanna Mustaparta. Her wisdom and intuition have been reassuring in hectic times, and she has been an important motivator during the work of this thesis.

Trondheim, 14th of July 2011

Nicholas H. Kirkerud

ABSTRACT

In the sensory systems of insects, the primary olfactory centre in the antennal lobe has been one of the major areas of interest for the last two decades. Considerable progress has been made in understanding this earlier part of the olfactory network, whereas very little is known about the odour processing of the higher order centres within the protocerebrum. In this study, the olfactory system of the moth *Heliothis virescens* was employed as a model. Intracellular recordings and stainings of neurons in the higher order olfactory centre in the lateral protocerebrum (LP) were performed during stimulation with identified primary plant odorants and multicomponent blends. Neurons were visualized by scanning with confocal laser microscope and 3-dimensional reconstructions. In order to morphologically identify and characterize neurons in the LP, recontructed neurons were registered into a standard brain atlas that has been developed for this species. Two different analyses were performed on the obtained physiology. First, a cluster analysis revealed clear divitions with respect to different neurons interspike interval (ISI) distributions, thus indicating groups of neurons with different functional properties within the higher order olfactory network. Secondly, a novel method in which to quantify complex temporal response patterns was introduced. A t-test used to compare the quantified reponses to single odorants versus blends showed that the majority of neurons (~70%) in the LP responded stronger to multicomponent blends. This indicated a predominant synergistic interaction of plant odours in the higher order olfactory centre of *H. virescens*.

TABLE OF CONTENTS

INTRODUCTION

In evolutionary context the chemical senses, olfaction and taste, are considered as the oldest of our senses. They are crucial in all organisms for intake of food and in many animals for reproduction, protection from predators or in adaptation to the environment. Research on the neural mechanisms underlying these senses have been ongoing for many decades, with anatomical and electrophysiological studies giving substantial contributions to the knowledge of the functional organisation in the olfactory and gustatory systems (Lledo, Gheusi et al. 2005; Yarmolinsky, Zuker et al. 2009; Galizia and Rossler 2010). With the advances in molecular biology for the last two decades, the use of new tools have resulted in identification of the receptor proteins as well as the neural pathways by molecular marking of particular neurons (Buck and Axel 1991; Hildebrand and Shepherd 1997; Vosshall and Stocker 2007)

Principles of the olfactory system

In olfaction, the major research on neural mechanisms concerns the receptor neurons and the primary olfactory centres; the antennal lobes (ALs) in insects analogue to the olfactory bulbs (OBs) in vertebrates, where comparisons have revealed many similar morphological and functional principles as well as certain differences. The receptor neurons are bipolar neurons with the dendrite surrounded by mucus or lymph and the axon projecting directly into the primary olfactory centre of the brain. Here, they make dense synaptic contacts with second order neurons in spherical structures, glomeruli, which are found to be constant in numbers and relative positions in a species (Strausfeld and Hildebrand 1999). Within the glomeruli, the information is handled in a network of synapses formed with local interneurons (LNs) and projection neurons (PNs), the latter being the output neurons of the primary olfactory centres. In both the invertebrate and vertebrate systems, efferent neurons that modulate the neural activity are also present. Whereas in the OBs a second microcircuit exists between the output neurons (mitral cells) and local interneurons (granula cells), the glomeruli of the ALs in insects contain in principle all synapses, i.e. between the receptor neuron terminals, the LNs, the PNs, and the modulatory neurons. Another difference is that insect antennal lobes contain PNs that innervate a large number of glomeruli (multiglomerular PNs) in addition to the numerous uniglomerular PNs (Homberg, Montague et al. 1988; Ro, Muller et al. 2007).

In vertebrates and insects molecular biological studies have shown the presence of a species-specific number of olfactory receptor proteins, and that each olfactory receptor neuron (ORN) expresses only one type of them. Furthermore, each subset of ORNs, expressing the same receptor protein type, project in one or two specific glomeruli in the primary olfactory centres. This principle has been referred to as the molecular logic of the sense of smell (Axel 2005). In vertebrates the receptor proteins being metabotrophic exerts their effects via G-proteins when activated by an odorant. The major transduction pathway involves activation of adenylyl cyclase which produces cyclic AMP as second messenger that opens cation channels. Subsequent influx of ions, including calcium, results in opening of Ca^{2+}-activated chloride channels, which causes efflux of Cl^- down its electrochemical gradient. Thus, a combination of influx of cations and efflux of anions contribute to depolarization of the ORNs eliciting firing of action potentials (Fain 2003). In *Drosophila*, the 7-transmembrane olfactory receptor proteins are found to be inverted as well as co-expressed with the particular protein, OR83b, present in all ORNs. The two proteins form a complex, which is found to act as a ligand gated channel when stimulated with the odorant (Sato, Pellegrino et al. 2008). Whether this is the only mechanism present in insects, or the ORNs additionally use a G-protein gated transduction pathway is a matter of discussion (Larsson, Domingos et al. 2004).

The ORNs, each expressing one type of receptor proteins, support the electrophysiological results in several insect species. Both pheromone ORNs and plant odour ORNs are found to be sharply tuned to one primary odorant, with weaker response to a few secondary components, and can be classified into similar types (Shepherd 1985). For the plant odour system, this has been revealed in studies linking gas chromatography to electrophysiological recordings from single receptor neurons - particularly well studied in the moth *H. virescens* (Rostelien, Borg-Karlson et al. 2000; Rostelien, Stranden et al. 2005). In other studies, screening of odorants has indicated broadly tuned ORNs, both in insects and vertebrates (de Bruyne, Clyne et al. 1999; Buck 2004). Thus, the mechanisms for how the information about different odorants is encoded in the ORNs seem to differ between species. This means that the code to the brain about an odour is mediated by a labelled-line, an across-fiber pattern mechanism, or a combination of the two in different species.

Odour processing in the primary olfactory centre

As expected from the ORN projection patterns in the primary olfactory centres, each odorant is represented by a unique pattern of glomerular activity during stimulation, as has been shown by calcium imaging studies of insects as well as vertebrates (Mori, Nagao et al. 1999; Rubin and Katz 1999; Sachse, Rappert et al. 1999; Silbering and Galizia 2007). In *H. virescens* results from Ca^{2+}-imaging and electrophysiology of the pheromone system in males show that each pheromone component is represented in each of the glomerular units of the sexual dimorphic macroglomerular complex dealing with pheromones (Berg, Almaas et al. 1998; Galizia, Sachse et al. 2000) . Similarly, for the plant odour system in *H.virescens*, Ca^{2+}-imaging has indicated representations in one or two glomeruli for each of the few primary odorants tested (Skiri, Galizia et al. 2004; Skiri, Ro et al. 2005). Results from the well studied honeybee and Drosophila with Ca^{2+}-imaging show a clear representation of odorants in either one or a few glomeruli (Deisig, Giurfa et al. 2006; Silbering and Galizia 2007) , indicating that this is indeed a general principle in insects. In vertebrates more complex patterns of glomerular activation are evident, which seems to be due to the relatively broadly tuned receptor neurons of these evolutionary higher animals (Friedrich and Korsching 1997; Davison and Katz 2007).

The leading hypothesis of how the AL process odours, includes complex dynamical interactions of both spatial and temporal aspects between the different glomeruli (Abbott and Luo 2007). These interactions are thought to be mediated by the local interneurons (LNs). There are two distinct sets of LN's characterised, one excitatory (histaminergic or/and glutaminergic transmission), and another inhibitory (GABAergic) (Sachse and Galizia 2002; Barbara, Zube et al. 2005). During stimulation with an odorant blend, excitatory LNs excite the PNs they innervate simultaneously, thereby promoting synchronisation. On the other hand, fast GABAergic LNs that receive input from the activated glomeruli, laterally inhibit the PNs that they innervate. This inhibition is strong enough to effectively reduce noise from the glomeruli that are not strongly activated by the blend, but not strong enough to annul the excitation of the activated glomeruli. Thus the code that leaves the AL is the spatio-temporal activation of the respective glomeruli, whereas the rest of the PNs are relatively silent. The interglomerular processes are important in enhancing the contrast of odour representations, forming the output of PNs, and inducing synchronicity (Lei and Vickers 2008). Recent studies in the moth and the honeybee, have supported this hypothesis. LNs have been shown to respond with significantly shorter latencies to blends than PNs, thus they are capable of rapidly suppressing PN responses (Krofczik, Menzel et al. 2008; Kuebler, Olsson et al. 2011) . Krofczik et al. further demonstrated that the PNs of the two different tracts in the dual pathway found in

honeybees, display different temporally rate codes. The lateral PNs that first reach the LP and then the calyces, were mainly suppressed by blend stimuli. Whereas the median PNs that innervates the calyces prior to the LP, responded similarly as to the individual components of the mixture (hypo-additivity). Kuebler et al found in the moth *Manduca sexta*, that approximately half of the PNs responded with suppression, and the other half with hypo-additivity, which coincided with the findings in the honeybee. Whether similar response dynamics are present in *H. virescens* remains to be investigated, but preliminary studies indicate similarities (Løfaldli et al. unpublished results). The sum of these results, strongly indicates that the interneurons play an important role in increasing odour contrasts and facilitating synchronization among output neurons from the primary olfactory centre.

Processing in the more sparsely distributed multiglomerular PNs is not well known. They vary considerably concerning both numbers and density of innervated glomeruli (Ro, Muller et al. 2007). In the honeybee, the multiglomerular PNs respond synergistic (stronger) to blends compared to single components (Sun, Fonta et al. 1993). This also seem to be the case in *H. virescens* , although only a few stained mPNs have been physiologically tested with blends (Løfaldli et al. unpublished results). Their direct route to the LP provides an alternative or perhaps "dominant" pathway for blend information. It has been speculated that the multiglomerular PNs function as hard-wired devices that feed the LP with information about the presence of biologically essential compositions of odorants, that are innate to the respective species. Whereas the uPNs that projects to the calyces provides a more flexible pathway, that are prone to changes through experience based learning (Lei and Vickers 2008).

Output from the antennal lobe

In most insects, including *H.virescens,* the PN axons follow three major tracts from the AL to the higher order olfactory centres; the calyces of the Mushroom Bodies (MB), the Lateral Protocerebrum (LP) and the Superior Protocerebrum (SP) (Ro, Muller et al. 2007; Galizia and Rossler 2010). The majority of PNs, which are uniglomerular, follow the inner antenno-cerebral tract (IACT), sending several branches to the calyces and then extending to the LP. The majority of the considerably fewer multiglomerular PNs follow the medial tract (MACT) that projects in the LP and the SP, bypassing the calyces entirely. In moths and other insect species, the the third major outer tract (OACT), contain both uniglomerular and multiglomerular PNs, the ratio of which varies between species. In *H. virescens* as well as the honeybee and other species the OACT and IACT axons show a contra-directional projection pathway in the calyces of the MB and the LP (Muller,

Abel et al. 2002; Kirschner, Kleineidam et al. 2006; Ro, Muller et al. 2007). Except for the locust, having only mPNs, uPNs represent the majority of PNs in most insect species (Ignell, Anton et al. 2001; Galizia and Rossler 2010) .

Higher order processing and integration

Knowledge about the processing of odour information in the higher brain areas is very limited. Most studies concerns the Mushroom Bodies in Hymenoptera and Diptera, the two most prominent structures in protocerebrum, which are involved in learning and memory (Ito, Suzuki et al. 1998; Okada, Rybak et al. 2007). Much less is known about the functional importance of the lateral and the superior protocerebrum, showing less structural organisations in anatomical studies. However, the LP is considered an important integration centre for olfactory and other sensory modality information, containing neurons that provide direct output to the premotor centres in the thoracic ganglia, which are involved in control of flight and walking behaviour (Kanzaki, Arbas et al. 1991b). The superior protocerebrum is also assumed to be a site for sensory integration and premotoric decision-making (Lei, Anton et al. 2001). The LP and SP should be addressed as possessing overlapping higher order networks consisting of parallel pathways, like the multiple ACTs that originate in the antenna lobes. In order to effectively study the different components that constitute this comprehensive network, methods of physiological as well as morphological characterisations need to be adapted.

Recently, a specific study of the pheromone circuit in the *Drosophila* male brain has shown that only three synaptic steps are needed to process the olfactory signal and produce a signal in descending neurons (Ruta, Datta et al. 2010). Input from modulatory interneurons in AL and LP, in addition to non-olfactory sensory information from other brain centres, are presumably also affecting the premotoric output signals from the brain. The pheromone system is often considered as an innate or «hard-wired» pathway, which is more direct, or at least less prone to plastic modifications, than the plant odour system (Lei and Vickers 2008). In principle, these two subsystems may work in similar ways,as concerns population coding, and partly projecting information to the same integrative areas in the protocerebrum (Christensen and Hildebrand 2002). Possible modulatory overlap between primary and accessory olfactory information has been indicated in a study of *Helicoverpa zea* (a species closely related to *H. virescens),* suggesting an intricate mutual influence of the two subsystems (Ochieng, Park et al. 2002).

Interspike interval distributions

Particularly in higher orders of olfactory neurons in the protocerebrum the temporal firing pattern may play an important role in odour coding, which motivated analyses of interspike interval distributions (ISI) in this study. ISI distribution of a neuron is a probability distribution that displays the relative frequencies of each interval size. The approach is to define a proper bin size, which reflects how roughly one wants to separate the different intervals. With a bin size of i.e. 5 ms, the ISIs ranging from 0-5ms are sorted into the first bin, the ISIs ranging from 5-10ms are sorted into the second bin, and so on in a consecutive way. The interval counts dedicated to each bin are then divided by the total number of observed intervals to show the relative frequency or probability of encountering that specific interval anywhere in the recorded sample. For a satisfactory estimate, the total ISI count of the recording should be >1500, which corresponds to 2.5 minutes of recording in a neuron with mean firing rate at 10 Hz (Halliday 1998; Ostojic 2011).

What does the ISI distribution really tell us in the manner of the neurons properties? Most obvious, it tells us the bandwidth in which the neuron operates. In non-bursting neurons, the distribution of ISIs is expected to contain a single peak/mode. Neurons with strong bursting properties tend to display a bimodal distribution. Phenomena like calcium-produced spike bursting (Smith, Cox et al. 2000), sub-threshold resonance (Engel, Schimansky-Geier et al. 2008), and non-stationarities in parts of the recording (Ostojic 2011) , are known reasons for bimodality in ISI distributions. The absolute and the relative refractory periods are also reflected in the ISI distribution. There will be no intervals shorter than the absolute refractory period, and very few in the beginning of the relative refractory period, since a greater input is necessary to evoke a spike during this period. The ISI distribution increases steeply as the relative refractory period gradually decays, until it reaches its peak value. The peak, also referred to as the mode, is the interval that occurred most frequently during the recording, but is not necessarily the mean. Subsequent to the peak, the distribution of intervals declines exponentially to zero. This is due to the fact that when intervals increase beyond the peak/mode, the arrival of the next spike is triggered in principle by a random Poisson process, and the inter-event times are distributed along a single negative exponential curve (Halliday 1998).

Simulations have been performed on different neuron models, as the leaky integrate-and-fire LIF model, the exponential integrate-and-fire model, and a Hodgkin-Huxley-like model, where the nature of ISI distributions were studied by varying the amount of fluctuations in the input (Ostojic 2011). The fluctuation of input to a neuron was modulated by the balance between excitation and

inhibition. These computational approaches showed three fundamental properties of the ISI distribution under the modulation of input fluctuations: 1) Under weak fluctuations of input with average beyond the membrane's spike generating threshold, the neuron will fire periodically, which is reflected by a narrow and close to Gaussian ISI distribution; 2) Under intermediate fluctuations of input, the ISI distribution contains an exponential distribution (the tail) that describe most of the intervals, and an effective refractory period at the short intervals; 3) Under circumstances of strong fluctuations, the ISIs tend to become exponentially distributed with bursts. Another observed property was that the mean firing rate, or the first moment of the ISI distribution does not change the shape of the distribution. Instead the shape is dependent on the coefficient of variation (standard deviation divided by the mean), which is strongly associated with the amount of input fluctuations. These same results have been demonstrated experimentally, with dynamic clamp technique on cortical slices to inject fluctuating current on neurons and study their ISI distributions (Miura, Tsubo et al. 2007), as well as in *in vivo* recordings in the primate neocortex (Maimon and Assad 2009). And each of these studies concluded with the gamma distribution as being the preferable choice to resemble the ISI distributions.

The typical shape of ISI distributions, have been found to vary systematically between neurons in different cortical areas, with more regular firing (less variation in the ISI distribution) closer to the motor areas than the visual areas, and bursty spike patterns dominating in prefrontal areas (Shinomoto, Miyazaki et al. 2005; Maimon and Assad 2009; Shinomoto, Kim et al. 2009). Thus, this indicates that the ISI distribution is closely related to functionality of the respective area in which the neuron is located. Whether these characteristics are analogue in neurons of the insect protocerebrum remains to be investigated. In the present thesis, the ISI distributions of protocerebral neurons in *H. virescens* has been analysed, in order to investigate possible similarities or differences between the overall tendencies of their temporal firing.

Recent progress and problems to be addressed

The work of this thesis is considered as a part of an extensive research on the moth, *H. virescens,* which is an important agricultural pest insect. The group's joint concern is to explore different aspects of neural coding of both olfactory and gustatory information, in addition to the mechanisms of appetitive and aversive learning and memory. Albeit numerous studies in our as well as other international groups have shed light on the odotopic organisation in the antennal lobe, as well as

some principles concerning interglomerular interactions, neuromodulations and input-output relationships, much is yet to be accomplished when it comes to fully understand the coding mechanism in this primary olfactory centre. In *H.virescens*, identification of the primary odorants that specifically activate olfactory receptor neurons have given insight on how plant odour information is encoded in the olfactory receptor neurons (Rostelien, Stranden et al. 2005). Furthermore, by stimulating with the primary odorants and defined blends, in addition to taste stimulants while performing intracellular recordings and stainings, olfactory and gustatory neurons in the moth brain have been characterised (Løfaldli et al. unpublished). In addition, a standard brain atlas (SBA) for *H. virescens* have contributed greatly by enabling integration of neurons from single brains into a common framework. This is an invaluable tool in positioning identified neurons and exploring possible connectivities between them with the aim to identify neuronal networks and understanding how they operate (Kvello, Lofaldli et al. 2009; Lofaldli, Kvello et al. 2010). Thus, the SBA provides a platform, in which present and future data can be integrated in developing a digital interactive brain.

Whether the general rule is that insects only need to pick up the scent of a few relevant plant odorants, or if a more elaborate blend is needed to identify the plant and its developmental stage, is still unclear. This kind of studies require knowledge about the relevant odorants used by the insect species and how the information about these odorants are processed in the CNS. The present study of *H. virescens*, for which we know relevant plant primary odorants, concerns responses of single neurons in the lateral and superior protocerebrum to primary odorants and mixtures. The neurons are physiologically characterised by intracellular recordings during stimulation with primary plant odorants. By fluorescent dye injections, some of them are morphologically identified, reconstructed in Amira and registered into the SBA (one of which will be presented in this thesis). Two main problems were addressed. The first problem was to investigate whether the ISI distributions may serve as a physiological method in comparing and categorising the recorded neurons in the LP/SP regions. If neurons that are found to share morphological (i.e. similar input/output) and response properties also operate within equal frequency bandwidths, the estimated ISI distributions may be used in separating different parts of the olfactory network. The second problem was to statistically compare the responses to single odorants and blends in protocerebral neurons, in order to find principal differences between higher order neurons and the neurons residing in the primary olfactory centre of the antenna lobe. Accompanying these investigations is the procedure of relating the physiological properties with the morphology of the neurons.

A method in which to quantify the varying responses in different neurons was adapted during the analysis of the neural data. The method, Temporal Response Strength (TRS), sums up the bin-wise deviation from the estimated firing rate of the spontaneous activity within a temporal window directly following onset of the stimulus. Since responses in many of the analysed protocerebral neurons contain complex parts of both excitation and inhibition, this method was more effective in quantifying the differences, than a conventional spike rate analysis.

Hypotheses

1) The population of integrative neurons projecting within the lateral/superior protocerebrum can be functionally categorized according to their inter spike interval distributions

2) Integrative higher order neurons distinguish between single plant odorants and multicomponent blends in their response patterns

MATERIALS AND METHODS

Storage and maintenance of insects

Pupae of the moth *Heliothis virescens* (Heliothinae: Lepidoptera; Noctuidae) were imported from the Syngenta laboratory culture in Basel, Switzerland, and sorted based on sex in separated incubators (Refritherm 6E, Struers) on a phase-shifted LD photo period (14:10 hours) at 22° C and 70% humidity. As the adult moths hatched, they were transferred into cylindrical containers (approx. 3400 cm^2) with maximum 8 individuals in each, in which they were fed a 0.15M sucrose solution. Experiments were exclusively performed on 3-5 days old insects.

Preparation of odorants

Biologically relevant plant odorants were diluted in decade steps to 10^{-5} in hexane. The substances, 100µL of each solution, were applied to separate odourless circular filter papers (approx. 2cm in diameter). Hexane was evaporated by exposure to a slow nitrogen flow. The filter papers were then inserted into plastic tubes (100mm * 5mm) that were concealed by tight plugs. Twelve different combinations of the selected odorants (10^{-5} concentrations) in equal amounts were prepared in blended solutions. For these solutions, 100µL was applied on the filter paper, in the same way as with the single odorants. For control, filter paper with hexane was similarly prepared. The tubes were stored in a refrigerator at 4º C, and replaced at least every 1-2weeks, dependent on the frequency of use.

Electrophysiological recordings

The moths selected for electrophysiological experiments were mounted in plastic tubes and immobilized with dental wax (Kerr Corporation, Romulus, MI, USA) after a period cooling at 4°C. Cephalic scales on the insect heads were removed to reveal the cuticle, and the antennae bases were fixed to melted wax bridges in order to prevent movement of the antennae during intracellular recording. In principal, two dissection approaches were used to expose the brain area of interest in the lateral protocerebrum *(Illustration 1)*. The most frequently used approach (*dorsal dissection*), was by cutting a window in the cuticle surrounding the posterior part of left antennal base with a microknife. Removal of trachea, intracranial- and antennal muscle tissue with forceps and microscissors, provided a full view of the antennal nerve and the antennal lobe (AL), as well as a

partial view of the lateral protocerebrum. The other approach (*lateral dissection*) was more challenging, as it required partial or complete removal of the left eye, as well as the dorsolateral cuticle close to the left antenna. The lateral dissection gave an optimal view of the lateral protocerebrum. To successfully reach neurons in the lateral protocerebrum, we alternated between dorsal and lateral dissections, and varied the insert angle of the electrode. The glass electrodes used were pulled with a Flaming-Brown horizontal puller (P97; Sutter Instruments, Novato, CA, USA). The dye 4% tetramethylrhodamine-biotin dextran (Micro-Ruby; Invitrogen, Germany) were filled into the electrode tip with the help of capillary forces and back-filled with a 0.2M solution of potassium acetate. The resistance of the electrodes were in the range of (120-350MΩ).

To insert the microelectrode into the brain tissue, we either removed a part of the neurolemma with fine forceps, or perforated it with a sharpened tungsten needle. The electrodes were steered into the brain by a micromanipulator, and a chlorized silver wire (reference electrode) was inserted into the head capsule through the compound eye. Ringer solution (in mM: l50 NaCl, 3 $CaCl_2$, 3KCl, 25 $C_{12}H_{22}O_{11}$ and 10 TES buffer, pH 6.9) was applied regularly throughout the registration. Penetration of the neural membrane appeared as a negative deflection on the oscilloscope. The spontaneous activity of the neurons varied between neurons, from close to zero, to up to 40 Hz.
After the physiological registrations, iontophoretically dye injection was attempted, by applying a positive current (1-5 nA, 2 Hz) repulsing the positively charged micro ruby invitrogen molecules. For optimal neuron staining, the injection lasted typically 10-15 minutes. The electrode signal was amplified (Axonprobe-1A, multipurpose microelectrode amplifier, Molecular Devices, CA, USA), digitalized by a data acquisition unit CED (Micro 1401 mk II, Cambridge Electronic Design Limited, Cambridge, UK) and Spike2 (version 7, CED) was utilized as a recording software and analysing tool, with a custom written program script existing of stimuli codes and magnetic valve commands to control the odorant stimulation.

The antenna was exposed to a continuous airflow at 400 ml/min from a glass tube, directed towards the left antenna. The prepared odorant tubes were connected to a separate tube and also directed towards the antenna. Upon activation of the valve, an air-puff of 100 ml/min lasting 300 ms was lead through the odorant tube. A delay from the valve opening to the arrival of odour at antenna was estimated at approximately 150ms. Compensation for this delay was made in the spike2 script. 500ms prior to each stimulation as well as 10 seconds following onset were recorded. Unstable periods were thus left out of the recordings, and to avoid adaptation, the neurons got proper time to reset to spontaneous activity in between stimuli.

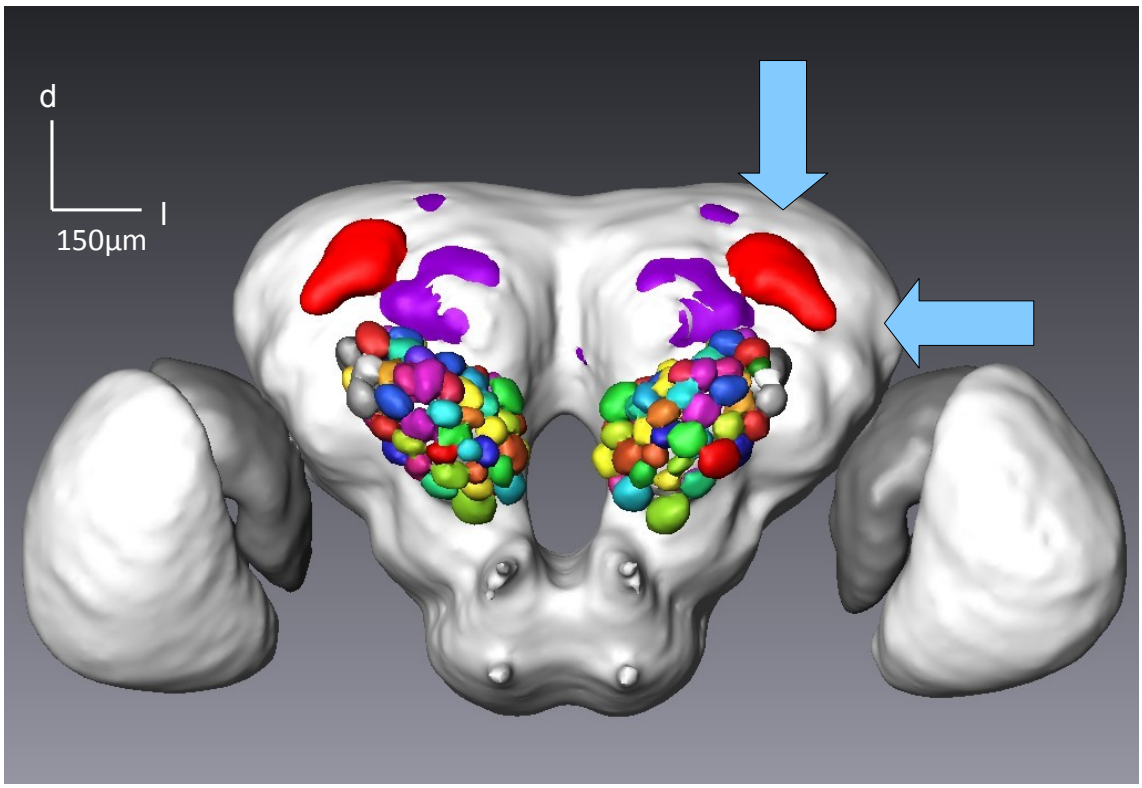

Illustration 1: Standard brain with arrows indicating areas of electrode insertions in the lateral and superior protocerebrum.

Initial investigation of odorant potency

Most of the neurons recorded from in the lateral and superior protocerebrum that responded to an odorant, also responded to at least one other odorant or blend. Therefore a comprimise had to be made in order to test as many odors and blends as possible, while offering the neurons enough intertrial time to avoid adaptation, and still get enough information for statistical analysis. In the early phase of this study, the most «potent» odorants and blends were decided through a broad spectrum testing procedure. The middle and late phase of the experiments thus contained the stimuli, that based on the early phase testings, were most likely to evoke a significant neural response. Some of the stimuli that were excluded through the early phase testing, were included infrequently during the middle and late phases, to ensure that these really were less likely to produce a response in protocerebral neurons.

Protocol

Brains in which neuron staining was attempted were dissected in ringer solution (in mM: l50 NaCl, 3 $CaCl_2$, 3 KCl, 25 $C_{12}H_{22}O_{11}$ and 10 TES buffer, pH 6.9) and fixed over night (4ºC) in 4% paraformaldehyde solution. This was followed by rinsing in a phosphate buffer solution (PBS in mM: 684 NaCl, 13 KCl, 50.7 Na_2HPO_4 and 5 KH_2PO_4, pH 7.2) for 10 minutes, and enhancement

with Streptavidin-Cy3 (Jackson Immunoresearch, West Grove, PA, USA; diluted 1:200 in PBS) either over night in fridge (4ºC), or 2 hours at room temperature. Subsequent rinsing in PBS and dehydration in an increasing series of ethanol (50, 70, 90, 96 and 100%; each for 10 minutes) made the brains ready for clearing with mehtyl salicylate. Preparations were mounted on custom cut aluminium plates in methyl salicylate with double sided cover glass, and studied under a fluorescent Zeiss bright field microscope (Axiovision Z1) for initial investigation of whether stainings were successful.

Stained preparations were rehydrated in a decreasing ethanol series (100, 96, 90, 70, and 50%; 10 minutes each) and rinsed in PBS solution, before they were dehydrated and degreased in xylol (5 min). Another step of rehydration followed by PBS rinsing was performed, and the brains were incubated for 30 minutes in collagenase (5mg/1ml PBS at 36ºC) . Washing with PBS (10 min), was followed by preincubation in a solution of 10% NGS (normal goat serum; Sigma, St. Louis, MO, USA) and 90% PBStx (PBS with 0.5% Triton X) for 30 minutes in room temperature. Brains were introduced to SYNORF1, a monoclonal antibody against synapsin. SYNORF1 (which was kindly provided by Professor E. Buchner, Würzburg, Germany) was diluted in PBStx (1:10) and 10% NGS. The incubation with the primary antibody lasted 48 hours in fridge (4ºC) . Rinsing in PBS followed, at six intervals, each lasting 20 minutes. Brain preparations were then introduced to a Cy5-anti-mouse secondary antibody (Jackson Immunoresearch) diluted 1:500 in PBStx solution, and incubated for 48 hours in fridge. A second 6×20minutes of PBS rinsing was then performed followed by dehydration with increasing ethanol series. Finally, the brains were again cleared and mounted on aluminium plates in methyl salicylate.

Visualization of stained neurons

For visualization of stained neurons, scanning of the brains was done with a confocal scanning laser microscope (Leica TCS SP5, Wetzlar, Germany) with a 10x air objective (HCX PL APO CS, 0.4 NA). 2-channel scannings at 488nm (Argon laser) to excite the micro-ruby dye, and at 633 nm (Argon laser) to excite the Cy5, were performed. Resolution of 1024x1024 pixels in the xy-plane, and a 2µm interslice distance were set a standards for overview scans (whole brain). The scans were stored as .lif files and converted to .am files in Amira 4.2 (Mercury Computer Systems, San Diego, CA, USA). Scaling of z-axis by a factor of 1.6 was done to compensate for refraction in methyl salicylate. Gauss-filtering and light intensity were adjusted to enhance the image of the stained neuron. Skeleton tool (Evers, Schmitt et al. 2005) was used to semi-automatically reconstruct the neuron. Following the reconstruction of the neuron, the neuropils surrounding the neuron that

corresponded with structures in the standard brain atlas were labelled and reconstructed as a surface file. This surface file was then affine-, and elastically adjusted to the standard brain atlas, in order to obtain new transformational parameters. These parameters were then applied to the reconstructed neuron. The procedure was similar to the one described by Brandt, Rohlfing et al. 2005.

Neurophysiological analyses

Spike sorting and filtering

The continuous voltage recordings of the neurons were processed with a wave form analysis (build in spike 2) that sorted out the spikes, based on a dynamic template-making algorithm. In most cases, the recordings contained similar waveforms that could be regarded as a single spike type. The recordings with two or more significantly different spike types were treated differently. Basically, the approach was to filter out the spike types that did not show any responses to the odour stimuli. Channels in which the spike waveforms were transformed to discrete time events were created for all neurons. The stimuli waveforms were transformed into a separate event channel. All data was then exported to MATLAB/Excel for further analysis.

Extraction of interspike interval data

Recordings that contained >1500 interspike intervals, at least 4 stimulations, and 2 responses per minute (in average) were included in the ISI cluster analysis. From the 39 neurons (20 different brains) with these qualifications, the ISI counts of the complete recordings were plotted in 5 ms interval bins from 0-250 ms. Prior to the cluster analysis, all interval bin counts were normalized (divided by total amount of spike intervals in the respective recording) in each neuron. Bimodal distributions were observed in a few cases, but only neurons with a unimodal ISI distribution were included in this analysis.

Extraction of temporal response comparison data

For further temporal response analysis, the criteria were stricter in order to find significant differences and similarities of odour representations. At least 4 response evoked stimuli of both single odorants and blends were needed in order to do a comparison test as described below. Additionally, each response to a specific odorant or blend had to be repeated at least twice. In order to get appropriate estimates of the air response, at least 3 repetitions were needed.

Cluster analysis

Multiple methods of agglomerative hierarchical clustering AHC (Statistics Toolbox, MATLAB® R2009a, The MathWorks, Natick, Massachusetts) were implemented upon the normalized ISI data. Five different distance algorithms were used to define distances between the neurons' ISI distributions in a multidimensional space, and 4 different linkage algorithms were used to construct dendrograms . The algorithms as well as the results from the individual approaches are shown in *Appendix I*. Neurons that tended to cluster together in the majority of approaches were placed together on the basis of: 1) The cophenetic correlation coefficient, that measured how accurate the dendrogram represented the actual correlations observed in the data set; 2) The inconsistency coefficients, which helped determine natural divisions among the ISI distributions. Closer descriptions of all methods of cluster analysis used are available at www.Mathworks.com

Distribution fitting

A distribution fitting analysis was performed on the ISI data set (each neuron's ISI distribution represented in bin counts) in *Distribution Fitting Tool* (Statistics Toolbox, MATLAB® R2009a). This tool adjusts a selected probability distribution to a vector of data by a maximum likelihood estimation, and suggests parameters accordingly. The gamma pdf [1] was selected as a preferred distribution, and goodness-of-fit was visualized for the different neurons in probability plots. Neurons defined in a mutual cluster through the earlier analysis, were represented in the same plot (*Figure 7*).The gamma pdf is,

$$f\left(x|k,\Theta\right)=\frac{e^{-x/\Theta}}{\Theta^{k}\Gamma\left(k\right)}x^{(k-1)}, \qquad \text{for } x\geq 0 \text{ and } \theta,k>0 \qquad [1]$$

, where $\Gamma(.)$ is the gamma function, k is the shape parameter, and θ is the scale parameter.

Temporal response strength (TRS)

With relatively few available responses per recording, a method in which to statistically quantify the responses was developed. Maximal frequencies in responses alone, is not enough to characterize the differences between responses to single odorants and blends. The main observed differences are the lengths and the temporal variations in the response spike trains. Essentially, the method that was developed is a way to describe a response as aggregated deviation from the spontaneous activity under a defined responsive window *(Illustration 2)*. First, it is dependent of an adequate estimate of

the spontaneous activity. This was done as a combination of three methods: 1) Total number of spikes divided on total recording time; 2) Exclusion of all response spike trains and then dividing the total number of spikes by the remaining recording time; 3) Evaluation of several windows between stimuli and averaging the frequencies. This procured three slightly different estimates from where the average was utilized. Response spike trains were arranged in three groups for every neuron: air (control), single odorants, and blends (≥9 odorants in equal concentrations). A proper response duration and bin size for each neuron was decided, based upon the temporal aspects of the responses. Typically, shorter bins quantify better responses of a neuron with high spontaneous activity and high frequent fluctuations than responses of a neuron with low spontaneous activity and stable phasic profiles. The response window was defined as the period from the stimulus onset, to the first bin where the five consecutive bins did not (on average) deviate significantly from the estimated spontaneous activity. PSTH of all responses were imported in excel, and a template sheet was constructed to perform the TRS calculations and following t-test, according to the principles explained below.

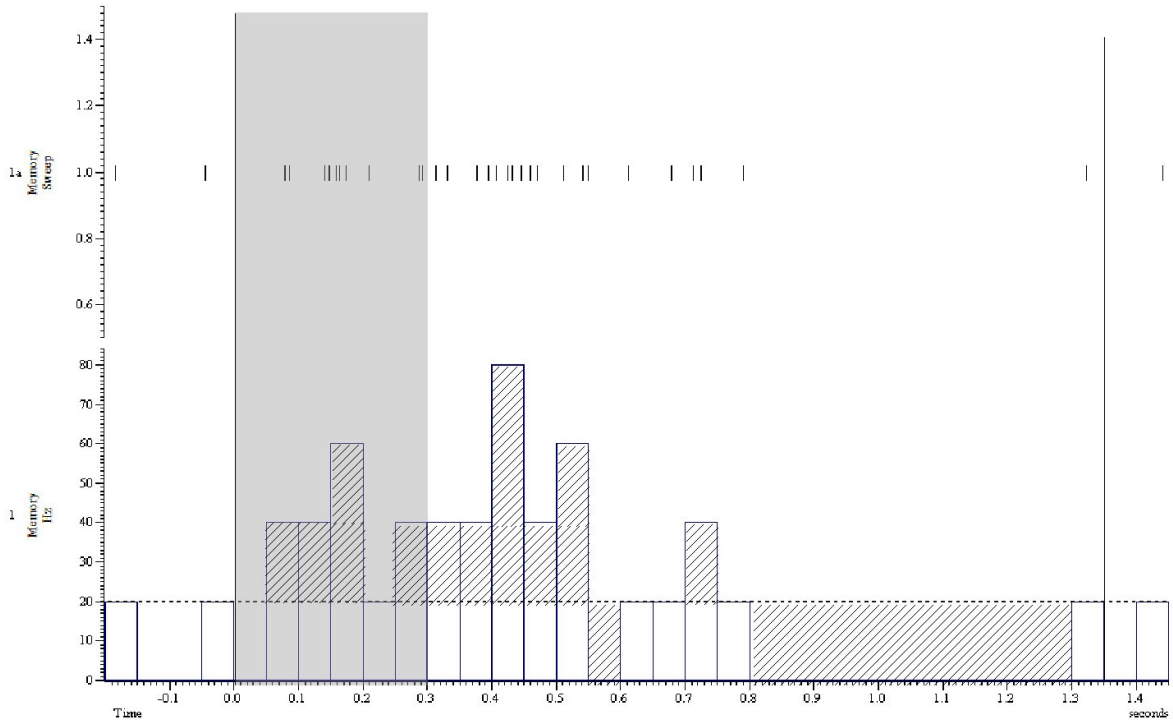

Illustration 2: Example of TRS calculation for an odour response in a protocerebral neuron. Raster plot (top) is translated into 50 ms bins of frequency (bottom). The response window is considered between the continuous vertical lines, and the shaded area indicates the stimulus window. All deviation from the estimated spontaneous activity (dotted line at 20 Hz) is marked with diagonal hatching, and illustrates the sum of the absolute values of differences as stated in equation [2].

Temporal Response Strength TRS, was calculated by

$$TRS = \frac{1}{n}\sum_{i=1}^{n} |r_i - r_{sp}| \qquad [2]$$

, where n is the number of bins within the response window, r_i is firing rate of bin i , and r_{sp} is the estimated spontaneous activity. The absolute value indicates that all deviation from the r_{sp} is counted as a positive contribution to the total response strength *(Illustration 2)*. This is crucial, because many of the neurons recorded from contained complex response profiles, containing both excitatory and inhibitory phases. However, since the level of spontaneous activity usually is closer to 0 than to the maximal firing rate, an inhibitory response tend to contribute less to the total response strength. In short, the TRS is a measure of the average binwise deviation from spontaneous activity within a defined response window.

The averaged TRS for a group of stimuli, was then characterized as

$$\overline{TRS} = \frac{1}{N}\sum_{j=1}^{N} TRS_j \qquad [3]$$

, where j is the response from the same group (control, singles, blends) of stimuli ranging in numbers from *1* to N, and TRS_j is the response strength for the j'th response as calculated in equation [2]. Variance within each group was calculated traditionally as

$$s^2 = \frac{1}{N-1}\sum_{j=1}^{N} (TRS_j - \overline{TRS})^2 \qquad [4]$$

To compensate for the part of the response explained by the neurons reaction to airflow, the estimated mean and variance of the response strength to the control-stimuli were subtracted from the response strengths (mean and variance) of both the single odorant and blend group. This approach depends on a sufficient number of control stimuli, in order to get a good estimate of how much of the deviation in the odour responses is due to mechanosensory stimuli or general fluctuations of the average firing rate r_{sp} unrelated to the odour stimuli.

Comparison of TRS to single odorants and blends

A two sample Students t-test was performed to explore differences between the two groups of responses. In occasions where the F-value (highest variance divided on lowest variance) did not exceed the F_{max}-value (alpha 0.05), a pooled sample standard deviation was used according to

$$s_x s_y = \sqrt{\frac{(n-1)s_x^2 + (m-1)s_y^2}{n+m-2}} \qquad [5]$$

where $s_x s_y$ is the pooled variance of responses from group x and y, while *n* and *m* are their respective sample sizes. The t-value was thus calculated as

$$t = \frac{\overline{x} - \overline{y}}{s_x s_y \sqrt{\frac{1}{n} + \frac{1}{m}}}, \text{ with } d.f. = n + m - 2 \text{ degrees of freedom.} \qquad [6]$$

On the rather few occasions where the F-value exceeded the F_{max} -value (alpha 0.05), the assumption of unequal variances was made in the estimation, and the t-value was calculated as

$$t = \frac{\overline{x} - \overline{y}}{\sqrt{\frac{s_x^2}{n} + \frac{s_y^2}{m}}}, \text{ with } d.f. = \frac{\left(\frac{s_x^2}{n} + \frac{s_y^2}{m}\right)^2}{\frac{(s_x^2/n)^2}{n-1} + \frac{(s_y^2/m)^2}{m-1}} \text{ degrees of freedom.} \qquad [7]$$

Assumptions of unequal variances tend to reduce the number of d.f.'s, thereby increasing the t_{max}-value and the p-value, making it tougher to reject the null hypothesis.

RESULTS

General descriptions of the protocerebral neurons

The results are based on data obtained from intracellular recordings of 62 neurons in the area of the lateral and superior protocerebrum. These include 39 neurons for which ISI analyses were made, 17 of them being in addition analysed in respect to temporal response strength (TRS) elicited by single compounds and mixtures. Two additional neurons were only analysed with respect to the latter method. *Table 1* contains and overview of how frequent responses to the different odorants and blends were obtained in the 62 neurons. Composition of the blends used can be found in *Appendix II, Table 4*. The number of neurons tested for each of the odorants differed, first of all because of the selection in the initial phase of odorants to be used in the successive experiments (described in the method), but also because of the variations in recording duration. Except for two blends (B1 and B11), the table shows a relatively higher percentage of responses to the other four blends (B2, B9, B10, and B12), than to the single odorants. Odorants that showed responses less frequently, were generally not tested as often, and contribute less to the weighted averages that are indicated in the table. The estimated difference between weighted averages for single odorants and blends is therefore likely to be smaller than the real average, meaning that the chance of evoking a response to single odorants is at least 10% lower than for blends. The odorants included in *Table 1* were tested more that 8 times. Five others tested occationlly are not included. It is also evident that the control (air puff from cartridge with evaporated hexane) often elicited responses in these neurons (58% of cases), but in general much weaker than to the odours. In some cases, the response to the airpuff had a shorter latency and seemed to constitue the initial part of the odour responses (not included in the statistical analyses).

In the electrophysiological recordings penetration of the neuron membrane appeared as a negative deflection (20-50 mV range), followed by spontanous action potentials (20-60 mV amplitude range). Responses to odours were recorded as excitation, inhibition or mixed excitation-inhibition. Examples of responses from 4 neurons (N6, N9, N22, N40) in *Figures 1-4* show a variaty of the observed firing activity in the 39 neurons. Responses to control, one odorant, and one blend, are presented for each of the four neurons demonstrating the complexity of responses that was typical for most of the recorded neurons. The presented data are unfiltered extractions of raw data from CED spike2. The timescales and voltage scales were adjusted in the presentations to accomodate the different spontaneous activities, temporal responses, and spike amplitudes of the neurons. The

stimulus window kept constant at 300 ms during all recordings are indicated.

Table 1: The primary odorants and blends used in a total of 62 protocerebral neurons. The number of neurons in which each odorant or blend was tested, as well as the percentage of neurons with responses to the respective odorant is presented. Control (air) was tested in all neurons, and elicited a weak response in approximately 58% of the cases. In general, single odorants evoked responses at an average of 81% of cases, as compared to 91% for the blends.

Odorants	**Nr of neurons tested**	**% responses**	**Blends**	**Nr of neurons tested**	**% responses**
3Z-Hexenylacetate	44	82%	B1	12	75%
Ocimene	12	83%	B2	19	95%
Linalool	27	89%	B9	22	91%
Geraniole	9	67%	B10	60	93%
E-verbenole	10	60%	B11	21	76%
Phenylethanol	45	89%	B12	47	96%
Germacrene-D	30	77%	**Weighted averages of probability for response:** Singles P(r): 0.81 Blends P(r): 0.91		
Farnesene	10	60%			
Control	62	58%			

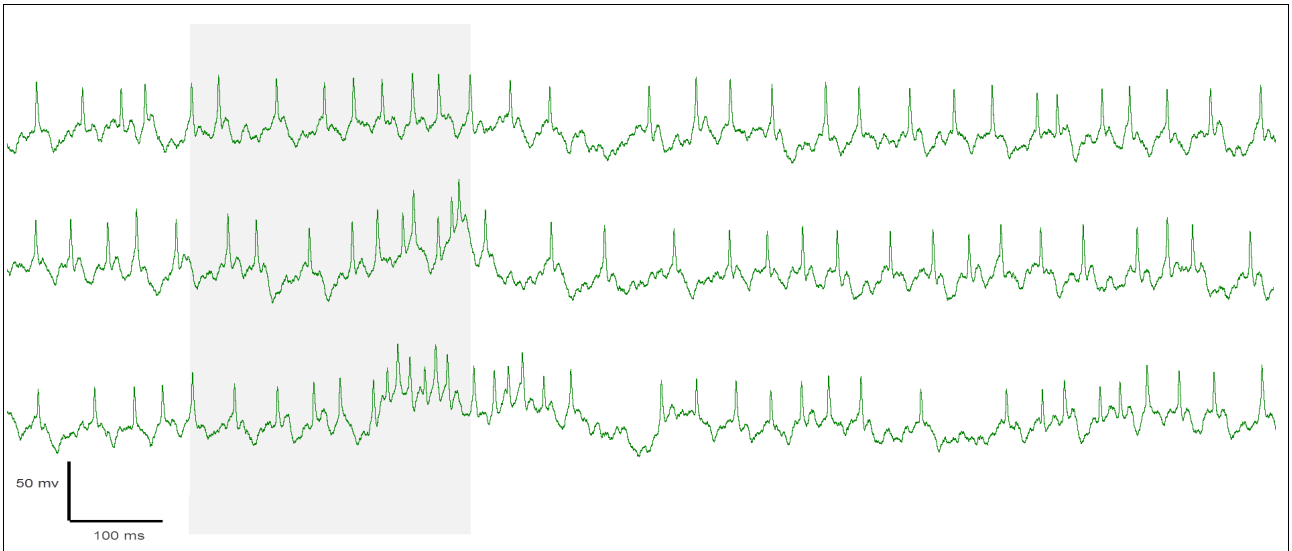

Figure 1: Example of responses from N22. Control (top); 3z- Hexenyl acetate (middle); 12-blend (bottom). Shaded area represents stimulus window.

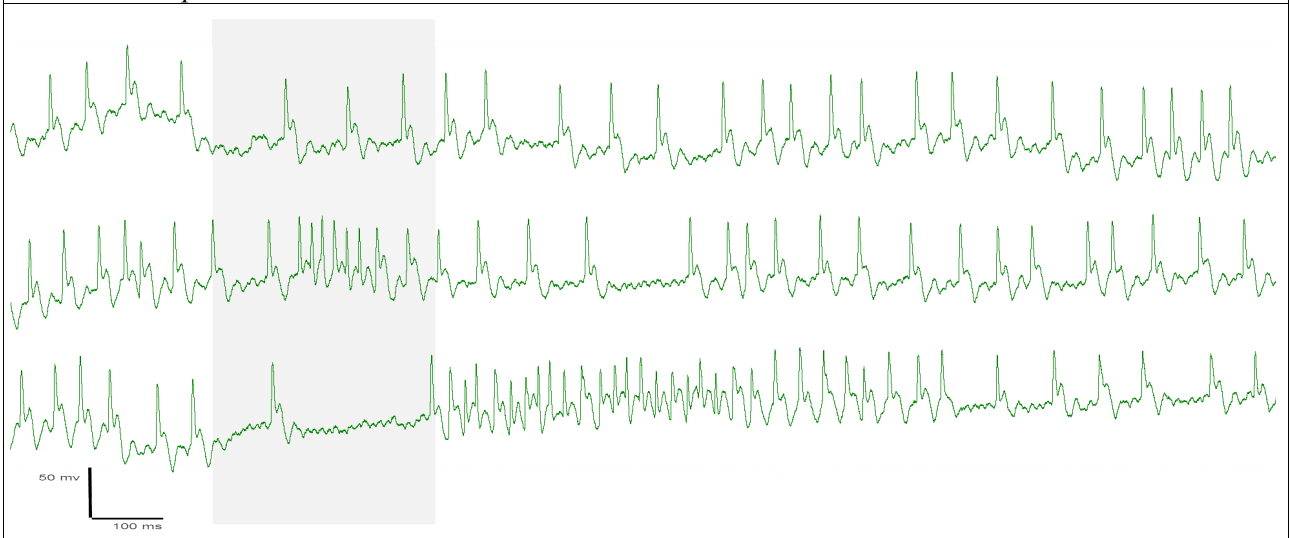

Figure 2: Example of responses from N6. Control (top); 3z- Hexenyl acetate (middle); 10-blend (bottom). Shaded area represents stimulus window.

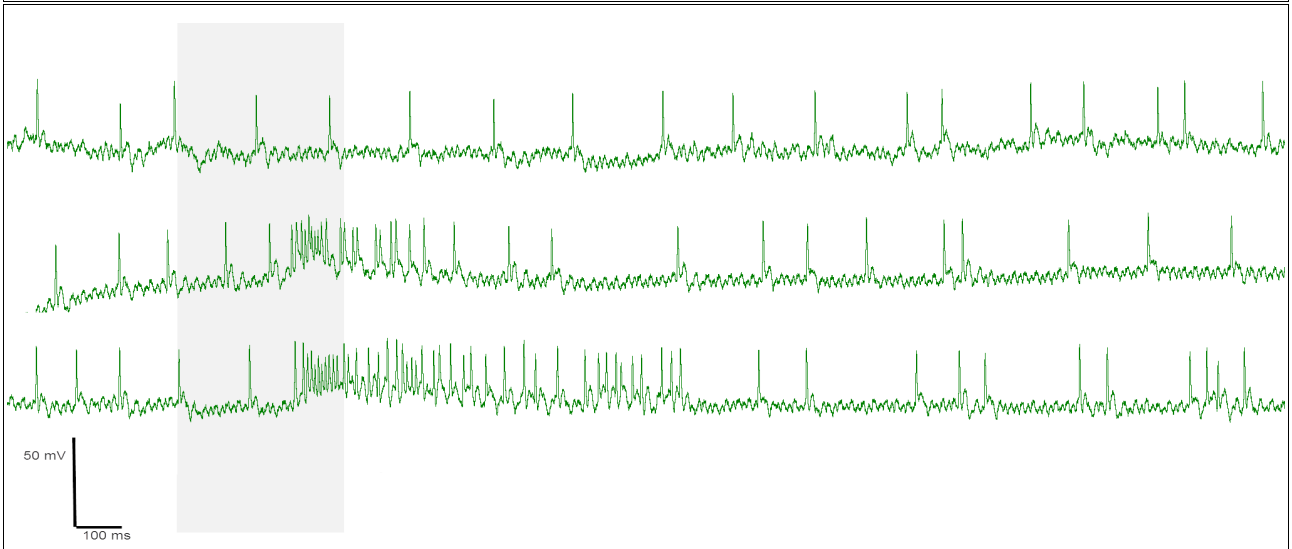

Figure 3: Example of responses from N40. Control (top);Phenyletanole (middle); 10-blend (bottom). Shaded area represents stimulus window.

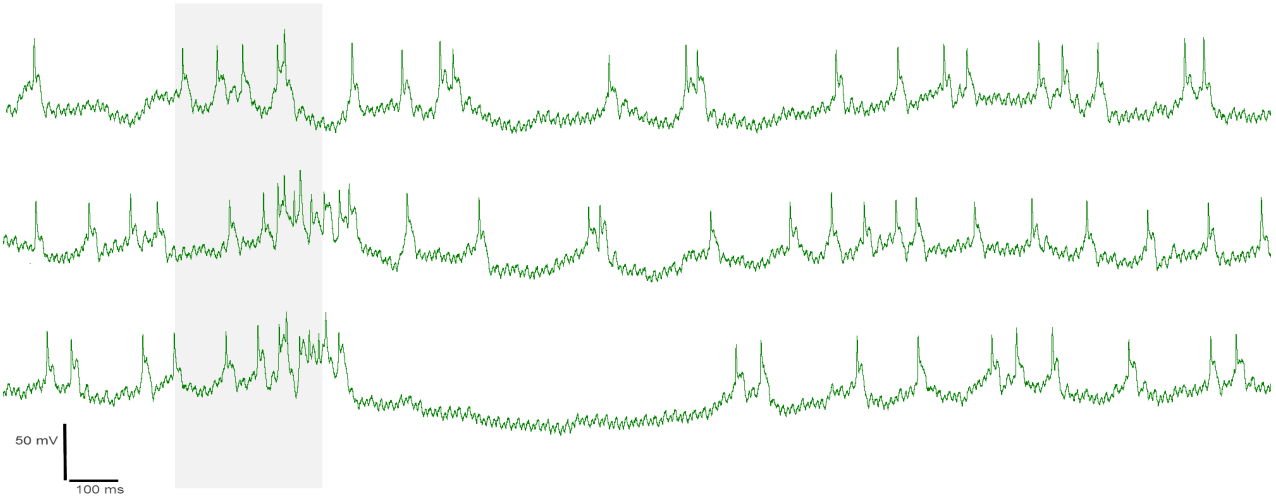

Figure 4: Example of responses from N9. Control (top);Ocimene (middle); 10-blend (bottom). Shaded area represents stimulus window.

Cluster analysis of interspike interval distributions

Five different distance algorithms were implemented to quantify differences and similarities between the ISI distributions of the 39 protocerebral neurons. Furthermore, 4 different linkage transformations (depending on distance algorithm approach) were used to construct 13 dendrograms *(Appendix I)*. Choice of clusters were based on inconsistency coefficients combinated with cophenetic coefficients and visual analysis of the dendrograms. Some variations in the results of the different approaches were observed, but the algorithms defined at least 5 distinct clusters with >4 members. The resulting clusters from the AHC analysis are displayed in a correlation matrix *(Figure 5)*, where neurons within each cluster have strong correlations of ISI distributions (>0.75 Correlation coefficient). Only 3 of the neurons were not dedicated to a cluster (N15, N18, N21). A summary of the neurons' cluster membership can also be viewed in *Table 3*.

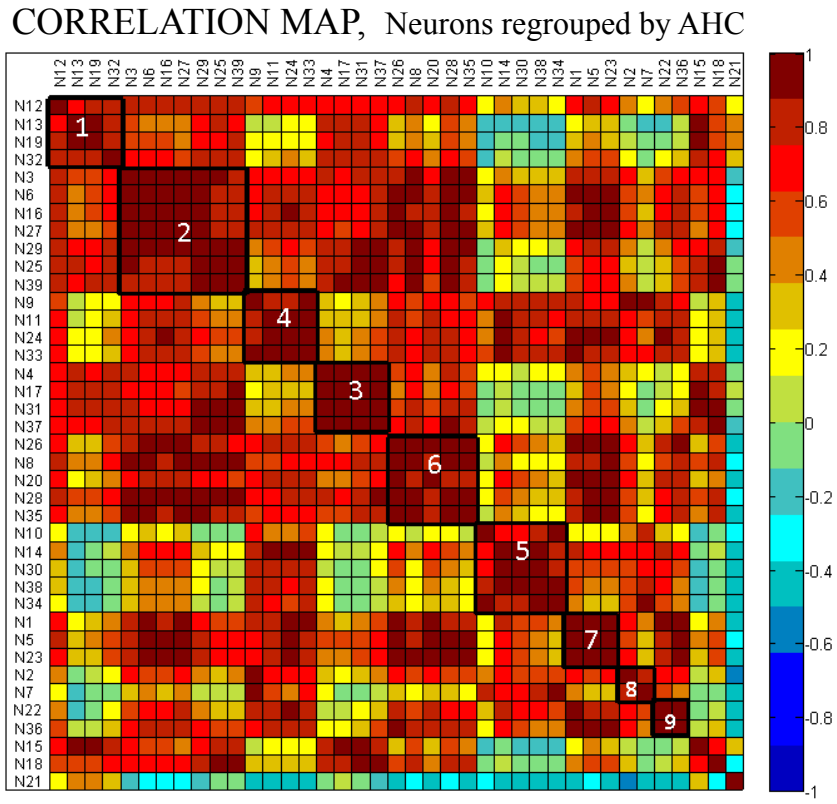

Figure 5: Correlation matrix of the 39 neurons after regrouping by 13 different combinations of agglomerative hierarchical clustering algorithms. Warmer colors indicate higher correlations (range from -1 to 1). Clusters with >4 neurons suggested by the algorithms are highligted by white numbers, (1-6); clusters with <4 neurons are higlighted by white numbers (7-9).

Gamma distribution fitting

Several distributions were fitted to the data, but none better suited than the gamma distribution when it came to goodness-of-fit (log-likelihood ratio test, results not included). This was expected, since ISI distributions tend to be governed by discrete Poisson events. When gathering gamma fitted curves from the ISI data of all neurons in one single plot, one would expect a gradually overlapping result, if assuming that there are no neurons of similar properties. However, this was not the case. Of the 39 neurons that were investigated, all except three had clear conformity with at least one other neuron. As could be concluded from the cluster analysis, 6 groups stood out, containing at least 4 neurons each *(Table 3)*. When sorted by these results, and having gamma distributions fitted, the obtained plots *(Figure 6, left column)* clearly illustrate the within-cluster similarities of the neurons. The goodness-of-fit plots show that the experimentally obtained ISI distributions generally fit the gamma distribution best at intervals smaller than 150 ms. Further, a weaker relationship was observed for neurons within cluster 5 than the rest (compare assemblement of the diagonal lines that represent the different gamma fits) *(Figure 6, right column)*. Within cluster 5, the ISI data also show a remarkably worse goodness-to-fit than for the remaining clusters. Thus cluster 5 seems to contain neurons with most variations, that have the weakest gamma fitted distributions.

The join plot of all the cluster means clearly shows that the ISI distributions of the different clusters are diversiformed *(Figure 7)*. Since the gamma curves of Cluster 4, 5 and 6 means are shifted towards the left compared to the rest, it is clear that they contain neurons that fire with higher spontaneous activity *(Table 2)*. However, cluster 5 have a much higher density in the small intervals than cluster 4 (or any of the other clusters), which is reflected in the low scale parameter and low variance for the gamma fitted mean curve *(Table 2)*. Dispersion of the goodness-to-fit probability curves *(Figure 7, bottom)* and ISI data from the different cluster means, indicate that none of the clusters means overlap significantly in any portion of the intervals.

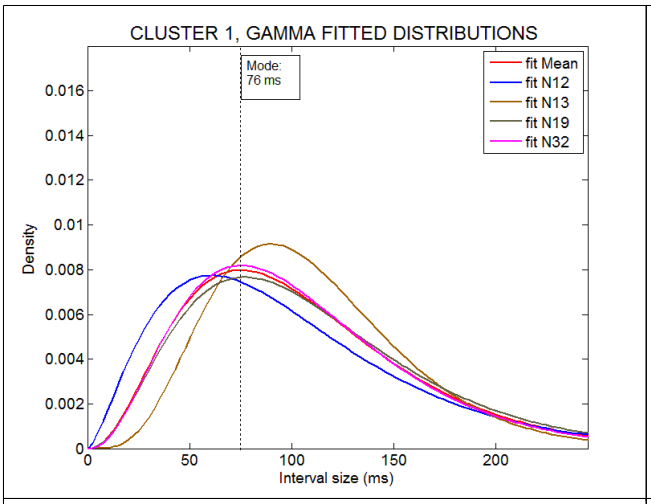
CLUSTER 1, GAMMA FITTED DISTRIBUTIONS
Mode:
76 ms
fit Mean
fit N12
fit N13
fit N19
fit N32
Density
Interval size (ms)

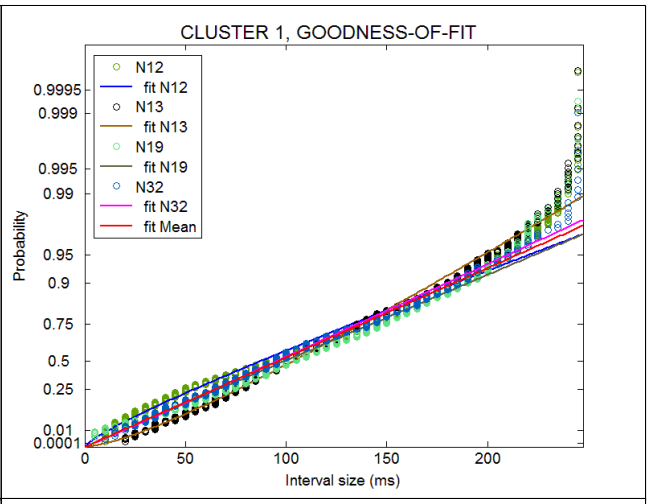
CLUSTER 1, GOODNESS-OF-FIT
N12
fit N12
N13
fit N13
N19
fit N19
N32
fit N32
fit Mean
Probability
Interval size (ms)

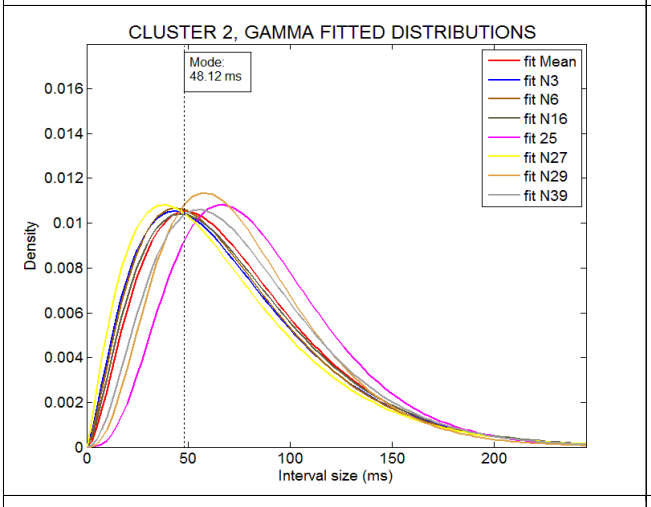
CLUSTER 2, GAMMA FITTED DISTRIBUTIONS
Mode:
48.12 ms
fit Mean
fit N3
fit N6
fit N16
fit 25
fit N27
fit N29
fit N39
Density
Interval size (ms)

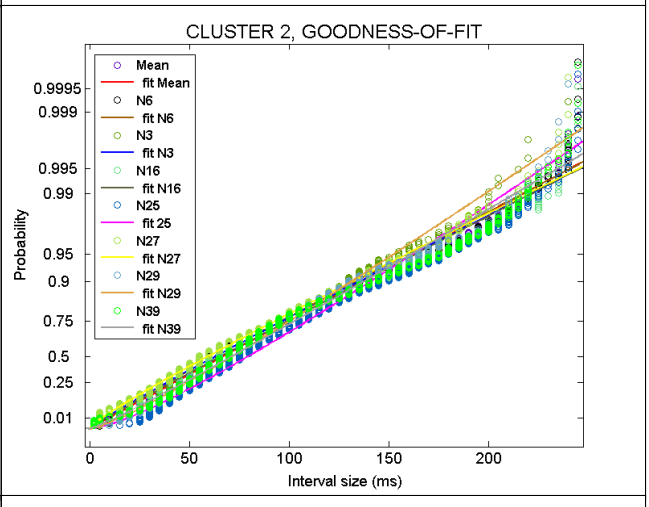
CLUSTER 2, GOODNESS-OF-FIT
Mean
fit Mean
N6
fit N6
N3
fit N3
N16
fit N16
N25
fit 25
N27
fit N27
N29
fit N29
N39
fit N39
Probability
Interval size (ms)

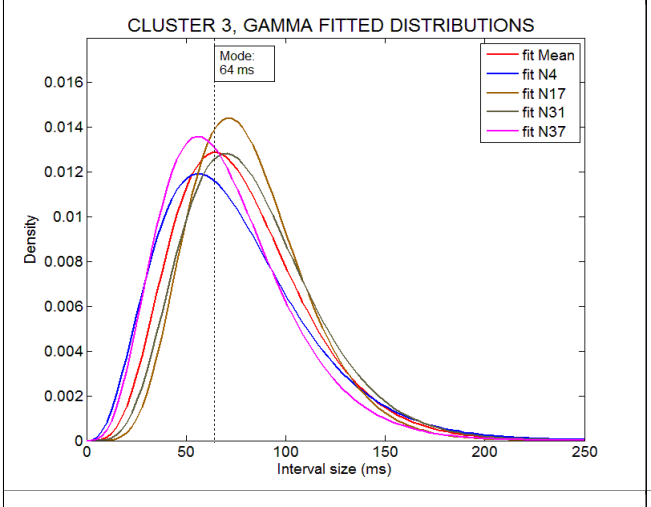
CLUSTER 3, GAMMA FITTED DISTRIBUTIONS
Mode:
64 ms
fit Mean
fit N4
fit N17
fit N31
fit N37
Density
Interval size (ms)

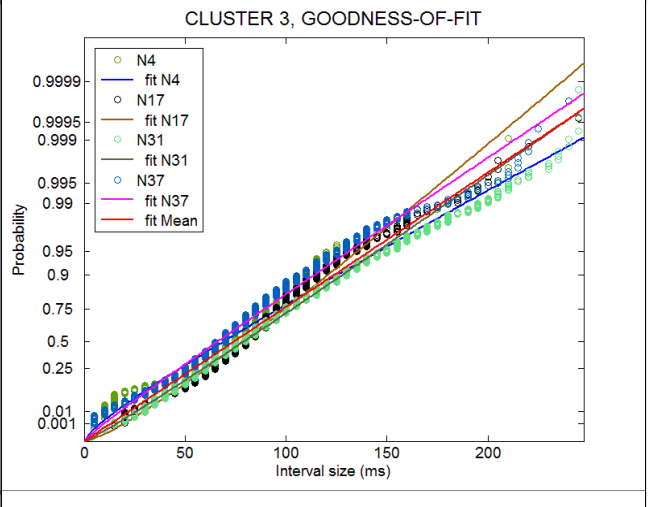
CLUSTER 3, GOODNESS-OF-FIT
N4
fit N4
N17
fit N17
N31
fit N31
N37
fit N37
fit Mean
Probability
Interval size (ms)

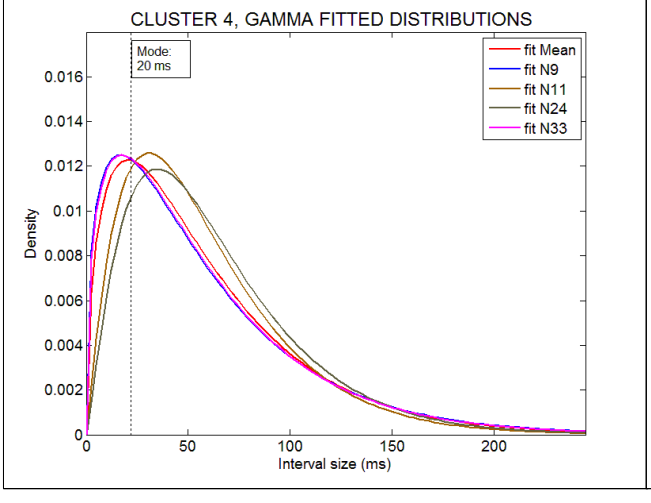
CLUSTER 4, GAMMA FITTED DISTRIBUTIONS
Mode:
20 ms
fit Mean
fit N9
fit N11
fit N24
fit N33
Density
Interval size (ms)

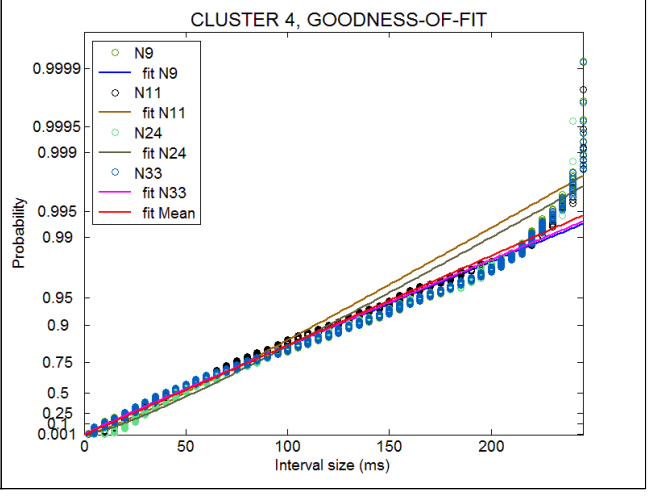
CLUSTER 4, GOODNESS-OF-FIT
N9
fit N9
N11
fit N11
N24
fit N24
N33
fit N33
fit Mean
Probability
Interval size (ms)

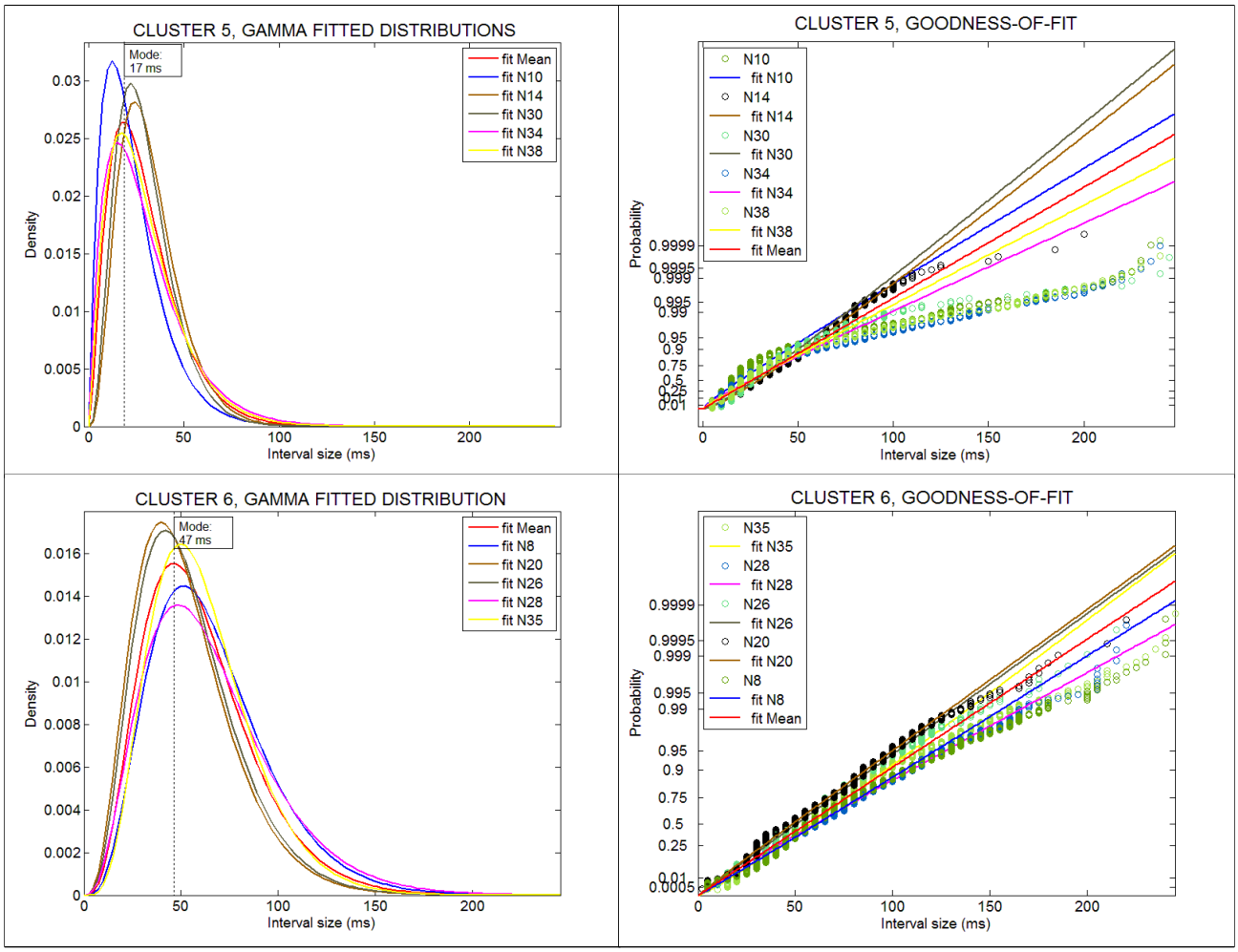

Figure 6: Left) Gamma distribution curves fitted to the interspike interval data from neurons in cluster 1 (top) to 6 (bottom). Median of the mean data gamma fitted curve is marked with a dotted line. Y-axis shows density, while X-axis contains the increasing interval sizes. Note that the Y-axis maximum of the cluster 5 plot is almost twice that of the other cluster plots; Right) Goodness-of-fit probability plots for interspike interval data to their respective fitted gamma curves of cluster 1 (top) to cluster 6 (bottom).

*Table 2: Numerical descriptions of gamma fitted distributions for the cluster means (Figure 7). Shape and scale parameters k and θ from the gamma distribution with estimated standard deviation. Larger k typically indicates more regular firing. Mean firing rate is calculated by 1/kθ * 1000ms.*

ClusterMean	k±stdev (shape)	θ±stdev (scale)	Mode	Mean	Variance	Mean Firing rate
C1	3.42±0.14	31.08±1.32	76.37	106.15	3299.17	9.4±1.58 Hz
C2	2.80±0.10	27.018±1.08	48.12	75.58	2041.94	13.2±1.94 Hz
C3	5.49±0.17	14.36±0.48	64.53	78.78	1130.88	12.7±1.64 Hz
C4	1.54±0.03	38.41±0.92	20.06	58.97	2265.05	16.9±1.46 Hz
C5	2.64±0.045	11.18±0.21	17.18	29.55	330.28	33.9±2.5 Hz
C6	4.41± 0.12	13.55±0.40	47.41	59.78	809.94	16.7±1.90 Hz

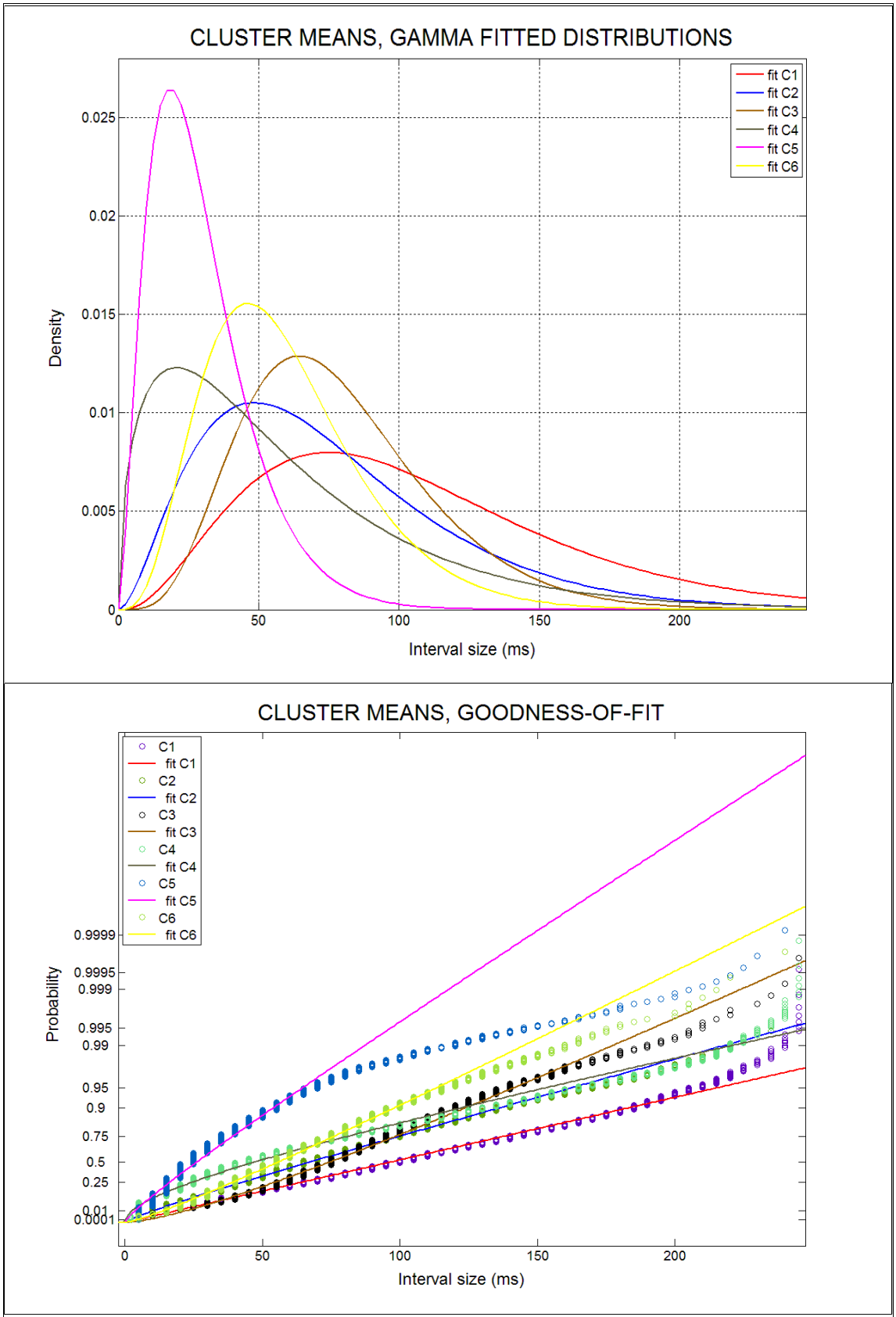

Figure 7: Gamma fitted curves of the ISI data means from cluster 1 to 6 (top); goodness-of-fit probability plots of the ISI data means to their respective gamma fitted distributions (bottom).

Temporal response strength of blends versus single odorants

From the 19 neurons that were selected for the t-test analysis 15 of them (~80%) were able to discriminate/distinguish between single odorants and blends. 13 of those (~70%) showed a significantly greater TRS for the blends, when compared with their TRS for single odorants *(Figure 8; Table 3)*. Four of the neurons showed no significant difference, three of which indicated a higher TRS for single odorants (N7, N15, N33) and one indicated higher TRS for blends (N15) *(Figure 8)*. Only two of the 19 neurons tested (~10%) had significantly greater TRS for single odorants than blends (N12, N41). The remaing 22 neurons from the ISI cluster analysis did not have enough repetitions of stimuli to significantly show any differences using classical statitical approaches. However, when inspecting these recordings, the impression is that the majority of neurons in LP and SP discriminate between single odorants and bigger blends. Examples of some of the differences that were typically observed between responses to single odorants and blends, are provided in PSTH diagrams *(Appendix II, Figure 11)*.

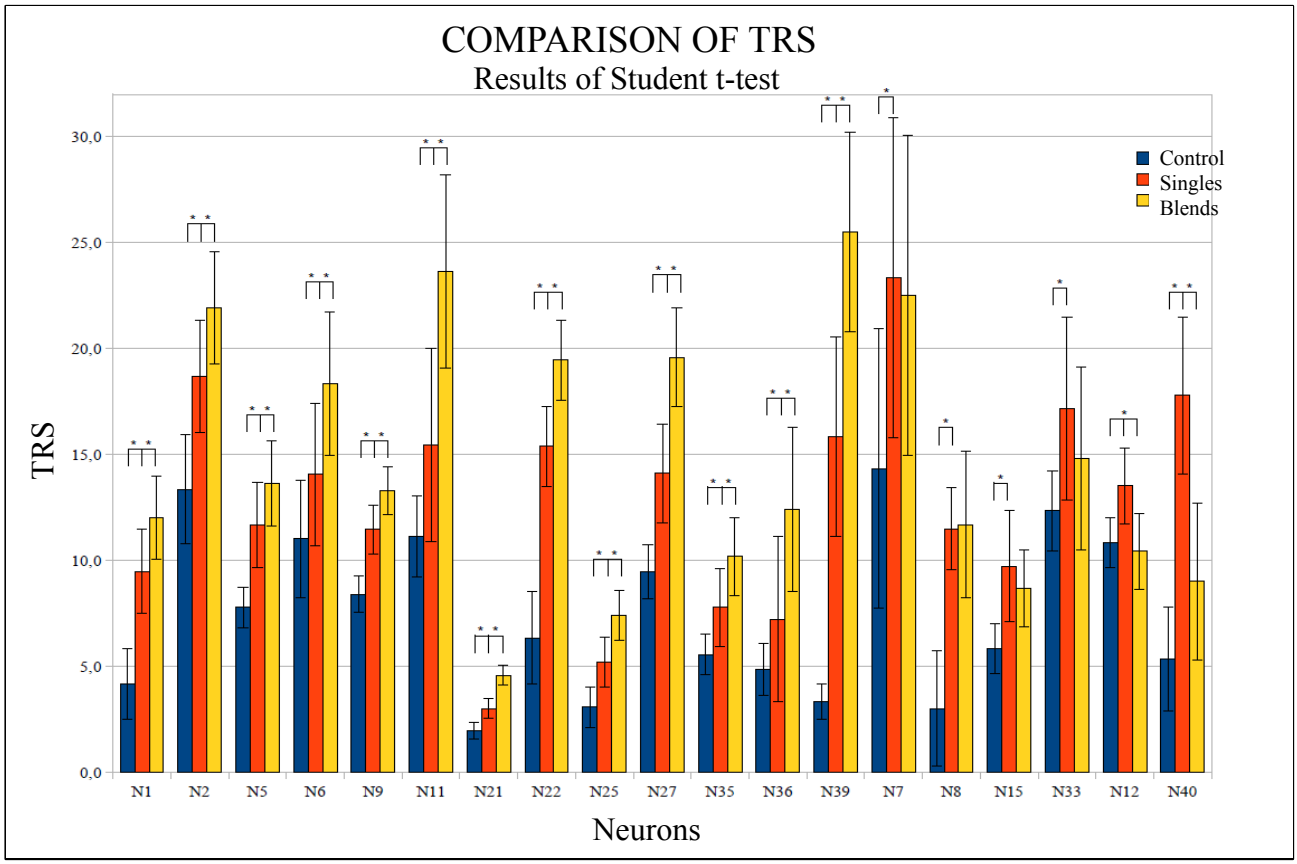

Figure 8: Student t-test results of TRS compared between control & singles, control & blends, and singles & blends in 19 protocerebral neurons. The columns indicate estimated TRS, which can be regarded as the average bin-wise deviation from spontaneous activity observed in the neurons' responses to either control, single odorants or blends, within a defined temporal window. Lines with asterisks located above the graphs indicate significant differenses of mean TRS ($\alpha = 0.05$).

Table 3: Summary table showing the 41 neurons inspected in either the ISI cluster analysis, the t-test analysis, or both. The reconstructed neuron N42, is also added. Neurons are arranged by the cluster membership assignments obtained by 6 different AHC algorithms. Clusters marked with asterisks contain less than 4 neurons, and were therefore not included in the gamma fitted figure (Figure 6). Neurons marked with NM had no cluster membership, while those marked with NA were not included in the ISI analysis due to low spike interval count. P-values from a t-test for comparisons of Temporal Response Strength between single odorants and blends in 19 of the 41 protocerebral neurons are specified, where B and S are abbreviations for TRS to blends and single odorants, respectively. The typical response firing pattern to each neurons is included; excitation (green), inhibition (red), and mixture (yellow).

Neuron	Dedicated Cluster	T-test p-values (α :0.05)			Resp. Firing	Neuron	Dedicated Cluster	T-test p-values (α :0.05)			Resp. Firing
		B>S	B≈S	B<S				B>S	B≈S	B<S	
N12	1			$1.6x10^{-2}$	mix	N30	5				mix
N13	1				exc	N34	5				mix
N19	1				exc	N38	5				inh
N32	1				inh	N8	6		0.41		mix
N3	2				exc	N20	6				inh
N6	2	$2.2x10^{-2}$			mix	N26	6				mix
N16	2				mix	N28	6				mix
N25	2	$8.2x10^{-4}$			inh	N35	6	$7.6x10^{-3}$			mix
N27	2	$1.1x10^{-3}$			mix	N1	7*	$1.6x10^{-4}$			exc
N29	2				mix	N5	7*	$3.2x10^{-2}$			mix
N39	2				mix	N23	7*				mix
N4	3				exc	N2	8*	$2.5x10^{-2}$			exc
N17	3				mix	N7	8*		0.38		exc
N31	3				inh	N22	9*	$1.5x10^{-2}$			mix
N37	3				exc	N36	9*	$2.9x10^{-2}$			exc
N9	4	$1.3x10^{-3}$			mix	N15	NM		0.23		mix
N11	4	$3.1x10^{-2}$			mix	N18	NM				inh
N24	4				inh	N21	NM	$1.3x10^{-6}$			inh
N33	4		0.14		exc	N40	NA	$9.2x10^{-3}$			mix
N10	5				mix	N41	NA			$1.8x10^{-3}$	exc
N14	5				mix	N42	NA				mix

Morphology of reconstructed neuron

The neuron N42 was one of the few in which a successfull staining was accomplished. It has an interesting morphology, in that it projects in the contralateral LP region of where it receives its input *(Figure 9)*. The dendrite covers a rather large area of the right LP, including the dorsolateral parts. The axon projects just ventral to the central complex and proceeds into the contralateral hemisphere, where it ends up in several branches with obvious blebs. The majority of the axonal branches are located more frontally, than the dendrites on the right side. A single soma was observed in the most lateral regions of the right (dendritic) side, but due to some damage in this region, it was not possible to trace the branch from soma to the dendrite. The neuron arborized proximal to the calyces on both sides, and possibly into the left calyx *(Figure 9E and D, single arrows)*. Two branches, also from the axon, stopped just prior to entering the left penduculus *(Figure 9D, double arrow)*.

Physiology of reconstructed neuron

N42 had almost no spontaneous activity, and did not fullfill the criteria for an adequate estimation of ISI distribution. Responses to both single odorants and blends were recorded in N42, but due to short recording time (started early staining), there were not enough repeated responses to conduct a t-test. The neuron responded with a brief burst of 3-4 spikes to control (air), and it is likely that the early burst in the responses to blends *(Figure 10)* was a result of mechanical input to N42. However, the rather late burst observed ~1200 ms post stimulus onset, was restricted to some of the single odorants and blends.

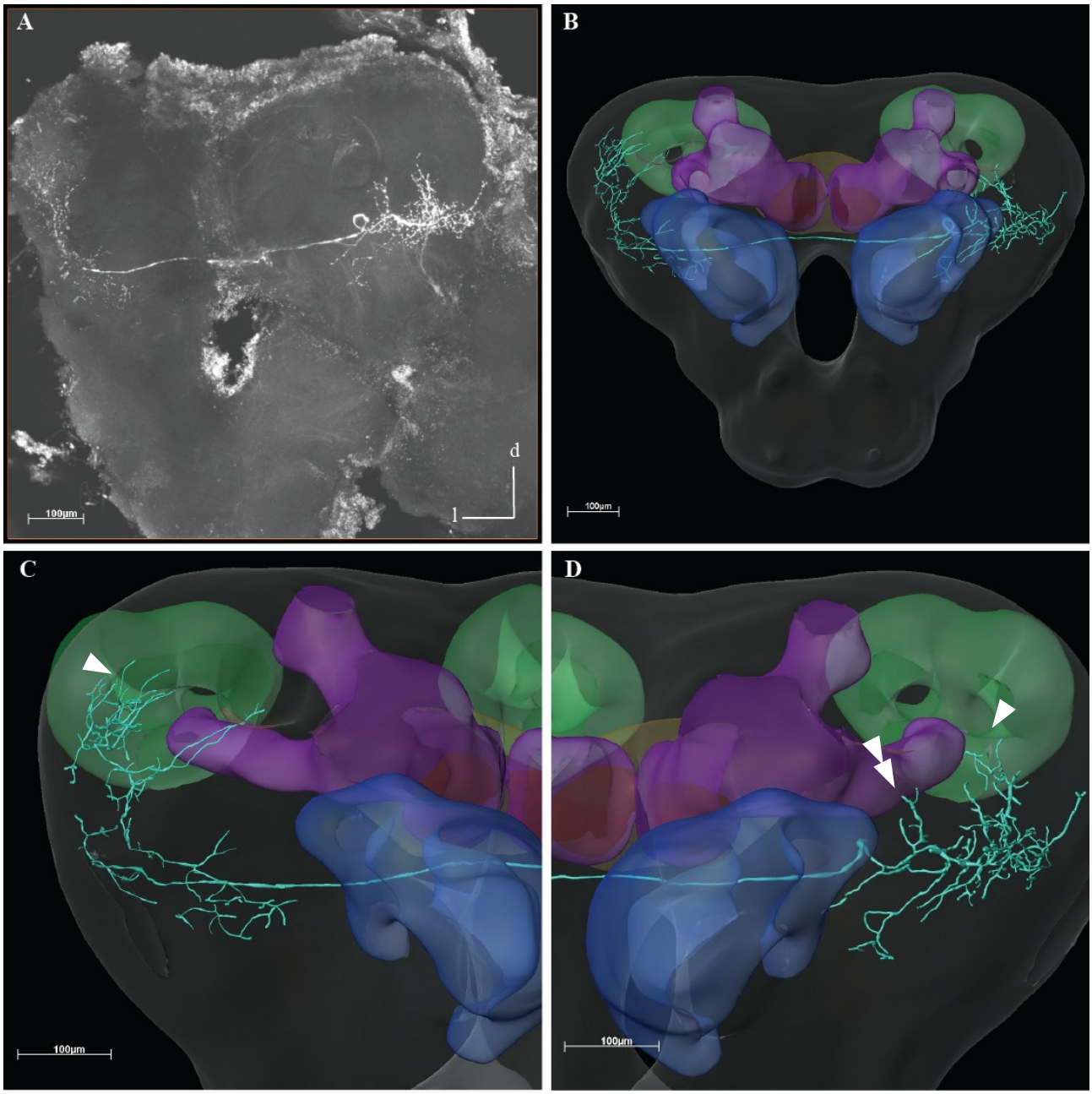

Figure 9: (A) Projection view of the raw data scan provided by the confocal microscope. (B) Frontal view of reconstructed neuron N41 registered into the SBA. Eye lobes removed. Dendrite is located in the right hemisphere. The axon branches which are situated more frontally compared to the dendritic branches, projects contralaterally into the lateral protocerebrum of the left hemisphere, with dense branching and evident blebs. This was the site of the intracellular registration. (C) Close-up of the right hemisphere and the dendrite. None of the branches innervate either the calyces, lobes or the penduculus of MB. (D) Close-up of the left hemisphere and the axonal projections. The most distal branches run close to the calyces and the penduculus, but did not clearly enter either of the neuropils.

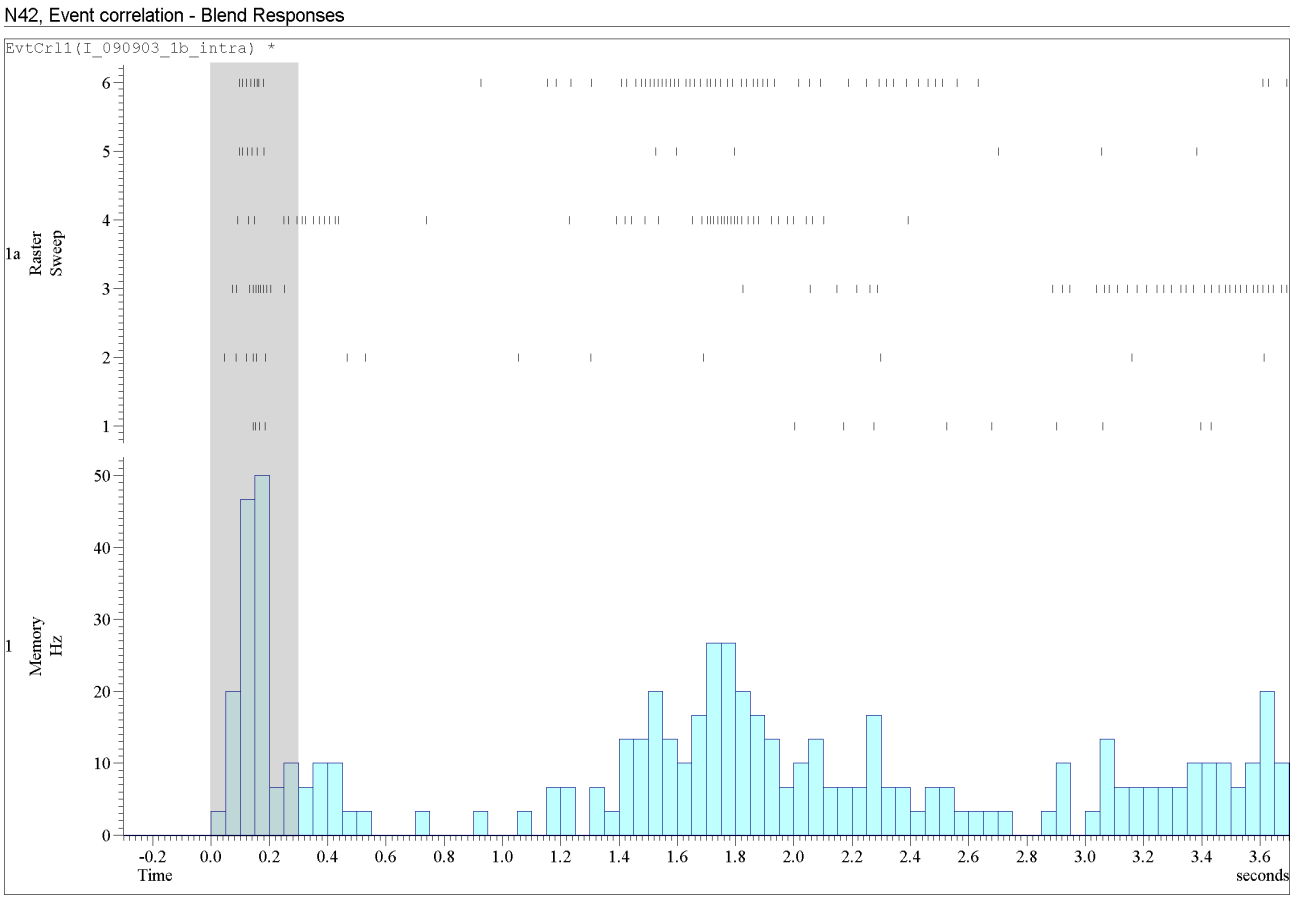

Figure 10: PSTH of responses to plant blends in the reconstructed neuron N42.

DISCUSSION

Biologically relevant odorants and blends have been used as test stimuli in only a handful of studies on protocerebral neurons in insects, all of which focused on pheromones (Kanzaki, Arbas et al. 1991; Kanzaki and Shibuya 1992; Lei, Anton et al. 2001;Lei and Vickers 2008). None of the studies concerned species in which the specificity for relevant plant odorants was known, like in *H. virescens*. The present study on higher orders of olfactory neurons in *H. virescens* had indeed the advantage that the plant odorants used as stimuli are biologically relevant, identified as primary odorants, each specifically activating one functional type of ORNs. This is important in resolving the two main questions in the present study: 1) Whether neurons in the protocerebral olfactory network can be categorised with respect to their ISI distribution, and 2) Whether these neurons distinguish between single odorants and blends. These questions were resolved by statistically analysing neurons from a selection of 62 recordings from the LP and SP that fulfilled the necessary requirements.

Although the 62 neurons were obtained in LP and SP, they may not necessarily all be neurons receiving information in the protocerebrum, but could also include PNs of the AL. Since successful staining was obtained in only a few of the recorded neurons, we do not know exactly how many of the recordings that belong to PNs of the AL. However, among the neurons morphologically characterised in this and the parallel ongoing studies in the lab, the majority of neurons recorded in the LP and SP were protocerebral neurons. In the AL most PNs are uniglomerular and therefore most frequently obtained in recordings from the AL, whereas only a few multiglomerular PNs have appeared. A simple hypothesis is that uniglomerular PNs, respond excitatory to stimulation with the primary odorant that activate the particular glomerulus, whereas multiglomerular PNs may respond by excitation to blends. From studies of the honeybee, *Apis mellifera* and the hawk moth, *Manduca sexta*, PNs were found to mainly respond in a phasic-tonic way lasting approximately for the duration of the applied stimuli (Krofczik et al. 2009; Kuebler et al. 2011). A particular multiglomerular PN in the AL of *H. virescens*, innervating many glomeruli and having axon in the medial ACT projecting to both the LP and the SP (recorded from the LP) showed excitatory response only to a multicomponent blend and not to the single odorants (Løfaldli et al., unpublished results). Most of the neurons in the present study showed complex response patterns with prolonged responses of either excitatory, inhibitory, or mixed character, the latter being the most common *(Table 3; Figure 1-4, 11; Appendix II, Figure 11)*. Compared to the PNs of the AL, it is possible that

higher orders of protocerebral olfactory neurons in general show more complex temporal response patterns than the PNs of the AL, reflecting that they receive converging input from many PNs as well as other neurons and encode the information over a greater time window.

From the 62 available recordings, only 39 (~ 60%) fulfilled the criteria set for the ISI analysis. The remaining 40% were either too short, contained too few responses, had particular low spontaneous activities, or a combination of these. If including more of the neurons lower levels of criteria had to be set, which would result in a decreased confidence of the ISI distribution estimations. A possibility considered during the analysis was that the responses influenced the shape of the ISI distributions, and since the number of responses varied from recording to recording, this could lead to significant changes in the resulting gamma fitted curves. In order to explore the impact of the responses on the estimated ISI distributions, pre-analysis removal of the spike trains following odorant stimulation were made for neurons in cluster 2 and 3, which had the two most similar cluster means *(Figure 7)*. By employing the spontaneous activity alone for these neurons, it was observed that the only impact on the gamma distributed curves, was a slight depression of the density of lower intervals, while the mode and exponential tail part remained the same. The goodness-of-fit were not noticeably altered. Thus the neurons within both respective clusters still had similar ISI distributions when excluding the responses (results not included). From this it was concluded that as long as the recordings contained approximately similar amount of responses per unit time, and fulfilled the other criteria set (explained in materials and method), the outcome of the cluster analysis would remain the same.

Furthermore, 19 neurons were selected for the TRS t-test analysis, with 17 of these also included in the ISI analysis *(Table 3)*. The results from the t-test in the present study indicated that the majority of neurons (~70%) fired synergistic, with stronger temporal responses to blends than to the tested single components. Hypo-additivity was shown in ~20% of the neurons, whereas significant suppression was only evident in 2 neurons (~10%). The trend of stronger responses to blends than to single components was evident in the majority of the other neurons as well, but due to few responses and repetitions the estimated response averages and variances would not be appropriate, and the t-test would not be credible in these cases. Since not all single odorants were tested in each neuron that responded to blends, one can not rule out the possibility that the blend response was really caused by one of the components. However, the majority of the neurons responded to several single components, and these responses were usually more similar to each other than to the blend responses. Thus it was assumed that the neurons in general did not respond in a hypo-additive way,

and that interactions between at least two components in a blend were responsible for the observed results.

The bilateral neuron that was reconstructed and presented in this thesis, N42, displayed some of the similar properties found in bilateral protocerebral olfactory neurons of other moths species (Kanzaki and Shibuya 1992; Lei, Anton et al. 2001). These neurons responded to pheromone stimuli, and projected more distinctly into the lateral accessory lobes (LALs), whereas N42 responded to plant odorants, and was located lateral and posterior to the LALs *(Figure 9)*. The response pattern of N42 showed two distinct bursts. The first with a short latency and duration, which was also present in stimuli to air, and a second longer-lasting burst present for some of the odorants and blends *(Figure 10)*. This extreme latency (~1200ms) has not been observed in any other protocerebral neurons so far, and could be an indication of slow bilateral interactions between the LPs being carried out by sparsely distributed neurons of this type. Unfortunately, there were not enough responses to compare TRS between single components and blends, and the almost non-existent spontaneous activity prevented a proper estimation of ISI distribution. When studied in the SBA together with earlier reconstructed neurons, it is obvious that N42 are closely associated with the 2nd order PNs. This neuron receives input from an area that overlaps with the output branches of recontructed uniglomerular PNs of the IACT, and provides output to the an area in the contralateral LP where input from muliglomerular PNs of the MACT are found (Løfaldli et al. unpublished). Bilateral connections between olfactory integration centres in the left and right hemisphere are thought to be crucial for the zig-zag searching behaviour observed in navigating moths following an odour plume (Kanzaki, Arbas et al. 1991a; Lei, Anton et al. 2001).

Implications of ISI clustering

The cluster analyses performed to find out whether the data exhibit a basis for placing the neurons into groups, resulted in clear clusters. The reason for preferring clustering methods when dealing with large amounts of data is that sorting by eye can be rather tedious and especially difficult when the data to be compared are somewhat similar. In the case of ISI distributions, the gamma fitted curves of two neurons often resemble each other at some parts (e.g. the peak), whereas differences are displayed in other parts (e.g. the tail). When dealing with these often subtle variations, it is advantageous to employ cluster analytical methods that quantify the differences and reveal complex relationships within the data. The problem with agglomerative hierarchical cluster (AHC) analyses is to select among several methods with varying resemblance to each other that gives somewhat different results *(Appendix I)*. A usual challenge is therefore to decide which methods are more appropriate and which are not for the data in question. Calculation of cophenetic coefficients and measures of inconsistency in the resulting dendrograms are helpful tools in making these decisions. They describe how well the different methods manage to represent similarities/dissimilarities among the variables (MATLAB R2009a). In the rather few occasions where a neuron fell between two clusters, (i.e. one half of the AHC algorithms place it in one cluster, the other half in another), the neuron's gamma curve was placed in both clusters, and a decision based on visual comparison was made. In three occasions (N15, N18, and N21), it was decided that the ISI distributions did not fit particularly well within any of the established clusters.

Of the 39 neurons treated with AHC methods, 29 were quite clearly belonging to six different groups with distinctive shapes *(Figure 6)*. Seven of the remaining ten neurons,were clustered into one group of three neurons, and two groups containing two neurons *(Figure 5; Table 3)*, all showing strong intragroup-relations among gamma fitted curves (gamma distributions not included). The 3 last neurons did not fit into any of the groups. One of these, N21, is morphologically identified as an output neuron from LP with inhibitory responses to the B10 blend (Løfaldli et al., unpublished results). None of the other 38 neurons in this analysis is identified as output neurons. However, since only a few are stained and reconstructed, the possibility exists that there are other output neurons among them.

Based on experimental data from different insect species, the concept of parallel olfactory processing has been proposed. Such a concept demands two or more signal pathways with neurons mediating different properties of an odour stimulus. The route through the Kenyon cells in the MBs for instance, relay the olfactory signal to extrinsic neurons, that connect with many other parts in the

protocerebrum, like output regions in LP (Okada, Rybak et al. 2007). These MB extrinsic neurons are known to alter their responses during conditioned learning of odorants, a property that could be reflected in their ISI distributions. From the results of the ISI data included in this thesis, one such MB extrinsic neuron, N3, with confined input in the beta-lobe and output in the LP (Løfaldli, unpublished results), was clustered together with 6 other neurons (cluster 2, *Table 3*). In 5 of these 6 cases, the electrode was deliberately targeted towards the penduculus and its lobes. Since only N3 was successfully stained and reconstructed, one incline to speculate whether some of the other 6 neurons in this ISI cluster also have input in the mushroom body lobes. There is a very low variation between ISI curves of the neurons in this cluster, and these neurons were dedicated equal cluster memberships by the majority of AHC methods *(Appendix I)*. The shape of the ISI curves, are not bimodal as found in the honeybee PE1 neurons, but more similar to the non-PE1 MB extrinsic neurons described (Okada, Rybak et al. 2007). However, another stained neuron, N40, with input in the beta-lobe, and output in the SP, showed a bimodal ISI distribution. It also displayed short response patterns with two distinct frequency peaks when stimulated with blends, and a considerable number of spike doublets and triplets were observed (*Appendix II, Figure 12 and 13*, morphology not included). These properties have also been observed in PE1 neurons in the honeybee (Okada, Rybak et al. 2007). This neuron had quite low spontaneous activity (6-10 Hz), and did not contain enough ISIs to be included in the ISI cluster analysis. In addition to the unclustered N40, all the 3 neurons tested within cluster 2 had a significantly greater TRS to blends than to single odorants. These results indicate that there could be different functional groups of MB extrinsic neuron, as have been found in the honeybee (Hänhel 2009). Further testing of the MB extrinsic neurons is needed to investigate the similarity of their ISI distributions, and to find out how well they discriminate between different odorants and blends.

Another stained and reconstructed neuron, N4, was clustered together with 3 other neurons (cluster 3, *Figure 6*). N4 has input in the LP, and output in the SP, providing a bridge for olfactory information between the two integration centres. As can be seen in the gamma distributions, the neurons in cluster 3 had relatively low spontaneous activities (12-14 Hz, *Table 3*). Looking at the part of the gamma curve where the responses contributed, it is also clear that cluster 3 had neurons showing some of the weakest responses. These neurons usually had responses that contained only short rises in frequency levels, followed by gradually decaying inhibition. When eradicating the response spike trains totally from the estimation of the ISI distribution, almost no change of the fitted gamma curves were observed (results not included).

The gamma distributions of neurons in cluster 5, are quite distinct in shape from neurons in the remaining clusters. Neurons in C5 clearly had the highest average firing rates (estimated 32-36 Hz, *Table 2*), and the most narrow distribution (smallest θ). This may indicate that these neurons either had a higher spike threshold and lower reset value; that they received inputs of weak fluctuations at a supra-threshold level, or a combination of the two (Ostojic 2011). However, this group clearly had weaker goodness-of-fit to gamma distribution compared with the other clusters, especially at the tail part *(Figure 7)*. The fitted gamma distributions in C5 neurons show that no intervals longer than 110 ms are likely to be observed, whereas the experimental data contain some sporadic counts of intervals beyond this size, thus causing a weaker fit in the tail parts of the respective gamma curves.

Contrary to neurons in cluster 5, the cluster 1 neurons had flat and elongated gamma shapes (high k, θ, and variance, *Table 2*). The exponential tail part has a small decay rate, reflecting the great variance of ISIs typical for these neurons. N12, was one of the two neurons found to respond significantly stronger to single components than to blends (suppression). The responses were quite similar in average maximum frequencies (~35 Hz for single components, ~30 Hz for blends), however the excitation for several single components lasted slightly longer, and were followed by a profound inhibition (~400 ms long) that was not observed in responses to the tested blends (results not included). These differences in responses did not appear when considering only the average frequency within the response window, as the profound inhibition neutrilized the longer excitation within the single odorant responses. This demonstrates the importance of evaluating the temporal response patterns in order to reveal particular differences. Similar traits were observed in the other neurons of cluster 1, but lacked the number of responses in order to show significant differences.

One may ask whether it is reasonable to assume that the ISI distributions reflect different functional groups of neurons within the olfactory network. In answering this question, the first argument would be that the ISI distribution is dependent on the key properties of a neuron, (e.g. in what frequency bands did the neuron tend to fire; absolute and relative refractory periods; threshold and reset potentials; leakage of current, etc.), and intuitively these properties should be quite similar in neurons that provide the same function in a network. This of course raises the more specific question of why neurons that share input and project onto common neurons should have similar ISI distributions. The second argument for defending an ISI clustering approach, is that if two neurons receive common input, they both need to be able to «read» the same olfactory code, and «translate» it to a common output signal dedicated for the same target neuron(s). If they have common input only, there would probably be room for more variations in how to convert the input, and the ISI distributions might vary somewhat. But when the two neurons in addition have common ouput, the

translated signal must be of a similar fashion in order for the target neuron(s) to be able to read and redistribute the code. How tight the temporal regime within which the different ouput neurons operate, is still largely unknown. When uncovered it will give valuable insight into how the olfactory network processes information. Simulations performed on common neuron models, have indicated that a neuron's ISI distribution is to a large extent dependent of the input fluctuations, thus suggesting that neurons receiving input from similar sources tend to employ ISI distributions of similar shapes (Ostojic 2011). Characterizations of the ISI distributions in AL neurons might reveal whether the ISI distributions of these second order neurons would fit into any of the clusters described in this thesis. Thus, it would have been interesting to analyse the data available in our lab on the antennal lobe PN recordings in *H. virescens*. However, the time limit for the thesis did not allow further analyses. For future studies this kind of analyses should be made for comparing ISI distributions of PNs in the AL with the data obtained in this thesis. In addition, comparison with data obtained in other species by international collegues should also be incorporated to elucidate the possible existance of common interspesific principles that might be ascribed to different parts of the olfactory network.

Characterizations of the different neurons' ISI distribution are valuable information in network simulations, as they reflect important properties that are essential for computational approaches. If further investigation supports the finding of characteristic ISI clusters of neurons with similar functions, it could certainly aid in the effort of building future olfactory network models. Additionally, establishing a database with integrated information about ISI distributions, morphology and response patterns, may provide a tool for interactive identification of neurons. In practice, this means that a script could be written (e.g. In spike2 or MATLAB), that produces an estimated plot of the ISI distribution during the *in vivo* recording. This information could then be automatically compared with established clusters, and provide feedback to the researcher indicating to neuron type. Thus, by implementing the ISI analysis interactively, prior knowledge might be accessed to optimize the search for neurons of interest. This is particularly valuable in unstable recordings from small brains, where it often is difficult to pinpoint electrode location to specific regions.

Limitations in intracellular recordings from small brains

A major challenge in intracellular recordings is to keep the recordings stable over a certain time to allow the number of selected tests to be performed before staining the neuron. The usual information theoretical and probabilistic methods for describing and comparing the responses, normally requires rather long lasting recordings, with few stimuli and several repetitions (Rieke 1997). In the present study we tempted to test 13 single primary odorants as well as 12 blends. Given that the recordings lasted 3-8 minutes, it was obviously unreasonable to expect results from the whole stimuli repertoire. Experiments with more elaborate dissections, like removing more of the cuticula, trachea and muscles, resulted in increased stability. However, this is also more intrusive, and takes longer time, possibly exposing the insects to more stress than necessary. For *in vivo* recordings, it is crucial to keep the animal as intact as posible, so that the investigated system is kept close to a natural state. The trade-off is unfortunately shorter recording times, and less stability. But with continously improving techniques and new equipment available, this picture is in the changing phase.

Comparison of TRS in single odorants versus blends

The t-test based on TRS indicates that there is a tendancy for neurons in the LP/SP to respond differently to single odorants and blends, in general with stronger responses to multicomponent blends than to single components. This is in contrast to results obtained from antannal lobe uniglomerular projection neurons (Krofczik et al. 2009; Kuebler, Olsson et al. 2011). In the present study, the p-values from the t-test are of a quite small magnitude for most neurons (>>0.05), suggesting a rather strong aptitude for seperation between responses to blends and single odorants in the majority of the tested neurons *(Table 3)*. Whether these results are applicable to the whole olfactory network in the these higher centra, or only confined to certain parts of the network, needs further invertigation. However, the neurons that showed significant differences in TRS originate from 6 of the clusters created in the cluster analysis (3 of them not included in *Figure 6*, because each of them have <4 members). This indicates that discrimination between single odorants and blends are found in neurons of *different properties*. Neurons N1, N21, and N39 which have been stained and reconstructed (Løfaldli et al. unpublished results), showed different morphology: One multiglomerular PN; one output neuron from the LP; and one mushroom body extrinsic neuron. Since each of the three respective neurons tested positively in the t-test (*Figure 8*), it implies that neurons from distinctly *different parts* of the olfactory network are able to discriminate between single plant odorants and multicomponent blends.

Aspects of the response quantification method

When a t-test on the same 19 neurons was performed where the highest frequency within the temporal response window served as the sole measure of response, significant differences ($\alpha = 0.05$) could be shown in only 2 of the respective neurons. Thus, the peak frequency alone, is not nearly as efficient in representing any given stimulus, as the Temporal Response Strength adapted in this thesis. The trapezoidal rule for calculating the average response in the temporal window, a method implemented by eg. Kuebler et al. 2011, was only tested in a few neurons. However, in this method, the inhibitive part of a complex (i.e. biphasic) response tends to neutrilize the overall excitatory response, thereby underestimating the actual deviance from spontaneous activity. There is no evidence in the olfactory system of insects, that the higher order integrative neurons actually utilise the average or maximum frequency of a temporal response. The investigations done in this thesis indicate that the TRS method is indeed more robust in olfactory coding neurons with complex response patterns (and probably neurons that code other modalities) than alternative rate quantification methods. This is because it quantifies the total change of frequency in a time window with respect to the spontaneous activity. Excitation as well as inhibition contribute to the total measure, thus the method avoids making implications of what part of the responses that is actually important for the postsynaptic neuron. The downside of the TRS method (as with other single measurement methods), is that it does not fully describe the temporal aspects of the response. That is, it lacks the description of the dynamical process in the response. Olfactory neurons in the LP/SP often show complex dynamical responses to odours, and especially to multicomponent blends. Considerable fluctuations in the frequency, varying latencies, and often bursts enveloped in inhibitive phases are prominent in higher order olfactory neurons. These characteristica are difficult to quantify when little data per neuron is available, but are probably important aspects of the olfactory code that need to be further investigated.

CONCLUSION

Cluster analysis indicated clear divitions in the ISI distributions among the different protocerebral neurons investigated. A selection of 39 neurons were divided into six clusters that each contained more than 4 neurons. Neurons within each cluster had high similarities in the gamma fitted curves of their ISI distributions. Responses to biologically relevant plant odorants and multicomponent blends were quantified by the Temporal Response Strength (TRS) method, which was introduced in this thesis. A t-test comparison of TRS to single odorants and blends indicated that the majority of neurons residing in LP and SP respond stronger to blends. This is in accordance with expected theories, but the results are novel for the plant odour system in insects. Most of the neurons recorded, displayed mixed responses that contained elements of both excitation and inhibition, which lasted considerably longer that the stimulus window. Long responses of mixed character, could be important characteristics for the third order neurons of the olfactory system, reflecting convergence of input from the AL projection neurons. Whether third order neurons receive and integrate multimodal information, and directly provide output to premotorneurons in the thoracic ganglia, or a fourth integrative step is needed, is yet to be confirmed. By categorizing neurons according to ISI distributions and temporal patterns, a physiological database can be integrated into the morphological platform established by the SBA. Combination of physiological and morphological descriptions, can be utilized in computational approaches, which are essential in understanding the complex principles of higher order protocerebral networks. An established database might be accessed interactively during physiological experiments, and provide information that facilitates the identification of specific neurons within the network, thus saving precious time associated with *in vivo* recordings. Since little is known about the network mechanisms behind transformation from sensory information to decision making and behaviour in the CNS, further physiological and morphological studies are needed to answer these fundamental questions. An experimental set up including odorant stimulation, intracellular recordings from protocerebral neurons, and electromyograms of thoracic neurons controlling flight-kinetics, would be ideal to study the complete pathway from the antenna to the wings. Understanding how third order neurons integrate multimodal information, and how this code is transmitted out of the brain in the descending neurons, will lead neuroscientists in the field to the next level in linking sensory stimuli with adequate behaviour.

ABBREVIATIONS

IACT – Inner Antenno-Cerebral Tract

MACT – Medial Antenno-Cerebral Tract

OACT – Outer Antenno-Cerebral Tract

AHC – Agglomerative Hierarchical Clustering

AL – Antennal Lobe

ISI – Interspike Interval

LAL – Lateral Accessory Lobe

LN – Local Interneuron

LP – Lateral Protocerebrum

MB – Mushroom Body

OB – Olfactory Bulb

ORN – Olfactory Receptor Neuron

uPN – uniglomerular Projection Neuron

mPN – multiglomerular Projection Neuron

PSTH – Post-Stimulus Time Histogram/ Peri-Stimulus Time Histogram

SBA – Standard Brain Atlas

SP – Superior Protocerebrum

TRS – Temporal Response Strength

REFERENCES

Abbott, L. F. and S. X. Luo (2007). "A step toward optimal coding in olfaction." Nat Neurosci **10**(11): 1342-1343.

Abel, R., J. Rybak, et al. (2001). "Structure and response patterns of olfactory interneurons in the honeybee, Apis mellifera." J Comp Neurol **437**(3): 363-383.

Adrian, E. D. (1953). "Sensory messages and sensation; the response of the olfactory organ to different smells." Acta Physiologica Scandinavica **29**(1): 5-14.

Axel, R. (2005). "Scents and sensibility: a molecular logic of olfactory perception (Nobel lecture)." Angew Chem Int Ed Engl **44**(38): 6110-6127.

Barbara, G. S., C. Zube, et al. (2005). "Acetylcholine, GABA and glutamate induce ionic currents in cultured antennal lobe neurons of the honeybee, Apis mellifera." J Comp Physiol A Neuroethol Sens Neural Behav Physiol **191**(9): 823-836.

Berg, B. G., T. J. Almaas, et al. (1998). "The macroglomerular complex of the antennal lobe in the tobacco budworm moth Heliothis virescens: specified subdivision in four compartments according to information about biologically significant compounds." Journal of Comparative Physiology a-Neuroethology Sensory Neural and Behavioral Physiology **183**(6): 669-682.

Bernays, E. A. and R. F. Chapman (1994). Host-plant selection by phytophagous insects. New York, Chapman & Hall.

Brandt, R., T. Rohlfing, et al. (2005). "Three-dimensional average-shape atlas of the honeybee brain and its applications." Journal of Comparative Neurology **492**(1): 1-19.

Buck, L. and R. Axel (1991). "A novel multigene family may encode odorant receptors: a molecular basis for odor recognition." Cell **65**(1): 175-187.

Buck, L. B. (2004). "Olfactory receptors and odor coding in mammals." Nutr Rev **62**(11 Pt 2): S184-188; discussion S224-141.

Christensen, T. A. and J. G. Hildebrand (2002). "Pheromonal and host-odor processing in the insect antennal lobe: how different?" Curr Opin Neurobiol **12**(4): 393-399.

Davison, I. G. and L. C. Katz (2007). "Sparse and selective odor coding by mitral/tufted neurons in the main olfactory bulb." Journal of Neuroscience **27**(8): 2091-2101.

de Bruyne, M., P. J. Clyne, et al. (1999). "Odor coding in a model olfactory organ: The Drosophila maxillary palp." Journal of Neuroscience **19**(11): 4520-4532.

Deisig, N., M. Giurfa, et al. (2006). "Neural representation of olfactory mixtures in the honeybee antennal lobe." Chemical Senses **31**(8): E60-E60.

el Jundi, B. and U. Homberg (2010). "Evidence for the possible existence of a second polarization-vision pathway in the locust brain." Journal of Insect Physiology **56**(8): 971-979.

Engel, T. A., L. Schimansky-Geier, et al. (2008). "Subthreshold membrane-potential resonances shape spike-train patterns in the entorhinal cortex." Journal of neurophysiology **100**(3): 1576-1589.

Evers, J. F., S. Schmitt, et al. (2005). "Progress in functional neuroanatomy: precise automatic geometric reconstruction of neuronal morphology from confocal image stacks." J Neurophysiol **93**(4): 2331-2342.

Fain, G. L. (2003). Sensory transduction. Sunderland, Mass., Sinauer Associates.

Friedrich, R. W. and S. I. Korsching (1997). "Combinatorial and chemotopic odorant coding in the zebrafish olfactory bulb visualized by optical imaging." Neuron **18**(5): 737-752.

Galizia, C. G., S. Sachse, et al. (2000). "Calcium responses to pheromones and plant odours in the antennal lobe of the male and female moth Heliothis virescens." J Comp Physiol A **186**(11): 1049-1063.

Galizia, C. G. and W. Rossler (2010). "Parallel olfactory systems in insects: anatomy and function." Annual Review of Entomology **55**: 399-420.
Halliday, D. M. (1998). "Generation and characterization of correlated spike trains." Computers in biology and medicine **28**(2): 143-152.

Halliday, D. M. (1998). "Generation and characterization of correlated spike trains." Computers in biology and medicine **28**(2): 143-152.

Hähnel, M. (2009). “Characterization of Mushroom Body Extrinsic Neurons in the Honeybee Apis mellifera and Their Role in Learning and Memory Formation: A Calcium Imaging Study.” Available at: http://www.diss.fu-berlin.de/diss/receive/FUDISS_thesis_000000010073.

Hildebrand, J. G. and G. M. Shepherd (1997). "Mechanisms of olfactory discrimination: Converging evidence for common principles across phyla." Annual Review of Neuroscience **20**: 595-631.

Homberg, U., R. A. Montague, et al. (1988). "Anatomy of antenno-cerebral pathways in the brain of the sphinx moth Manduca sexta." Cell Tissue Res **254**(2): 255-281.

Homberg, U., S. Hofer, et al. (2004). "Neurobiology of polarization vision in the locust Schistocerca gregaria." Acta Biol Hung **55**(1-4): 81-89.

Hubener, M., D. Shoham, et al. (1997). "Spatial relationships among three columnar systems in cat area 17." Journal of Neuroscience **17**(23): 9270-9284.

Ignell, R., S. Anton, et al. (2001). "The antennal lobe of orthoptera - anatomy and evolution." Brain Behav Evol **57**(1): 1-17.

Ito, K., K. Suzuki, et al. (1998). "The organization of extrinsic neurons and their implications in the functional roles of the mushroom bodies in Drosophila melanogaster Meigen." Learn Mem **5**(1-2): 52-77.

Kanzaki, R., E. A. Arbas, et al. (1991a). "Physiology and morphology of protocerebral olfactory neurons in the male moth Manduca sexta." J Comp Physiol A **168**(3): 281-298.

Kanzaki, R., E. A. Arbas, et al. (1991b). "Physiology and morphology of descending neurons in pheromone-processing olfactory pathways in the male moth Manduca sexta." J Comp Physiol A **169**(1): 1-14.

Kanzaki, R. and T. Shibuya (1992). "Long-Lasting Excitation of Protocerebral Bilateral Neurons in the Pheromone-Processing Pathways of the Male Moth Bombyx-Mori." Brain Research **587**(2): 211-215.

Kirschner, S., C. J. Kleineidam, et al. (2006). "Dual olfactory pathway in the honeybee, Apis mellifera." J Comp Neurol **499**(6): 933-952.

Krofczik, S., R. Menzel, et al. (2008). "Rapid odor processing in the honeybee antennal lobe network." Front Comput Neurosci **2**: 9.

Kuebler, L. S., S. B. Olsson, et al. (2011). "Neuronal processing of complex mixtures establishes a unique odor representation in the moth antennal lobe." Frontiers in Neural Circuits **5**: -.

Kvello, P., B. B. Lofaldli, et al. (2009). "Digital, Three-dimensional Average Shaped Atlas of the Heliothis Virescens Brain with Integrated Gustatory and Olfactory Neurons." Front Syst Neurosci **3**: 14.

Larsson, M. C., A. I. Domingos, et al. (2004). "Or83b encodes a broadly expressed odorant receptor essential for Drosophila olfaction." Neuron **43**(5): 703-714.

Lei, H., S. Anton, et al. (2001). "Olfactory protocerebral pathways processing sex pheromone and plant odor information in the male moth Agrotis segetum." J Comp Neurol **432**(3): 356-370.

Lei, H. and N. Vickers (2008). "Central processing of natural odor mixtures in insects." J Chem Ecol **34**(7): 915-927.

Linn, C., M. Campbell, et al. (1991). "The Effects of Different Blend Ratios and Temperature on the Active Space of the Oriental Fruit Moth Sex-Pheromone." Physiological Entomology **16**(2): 211-222.

Lledo, P. M., G. Gheusi, et al. (2005). "Information processing in the mammalian olfactory system." Physiol Rev **85**(1): 281-317.

Lofaldli, B. B., P. Kvello, et al. (2010). "Integration of the antennal lobe glomeruli and three projection neurons in the standard brain atlas of the moth heliothis virescens." Front Syst Neurosci **4**: 5.

Maimon, G. and J. A. Assad (2009). "Beyond Poisson: increased spike-time regularity across primate parietal cortex." Neuron **62**(3): 426-440.

Meister, M. and T. Bonhoeffer (2001). "Tuning and topography in an odor map on the rat olfactory bulb." Journal of Neuroscience **21**(4): 1351-1360.

Miura, K., Y. Tsubo, et al. (2007). "Balanced excitatory and inhibitory inputs to cortical neurons decouple firing irregularity from rate modulations." The Journal of neuroscience : the official journal of the Society for Neuroscience **27**(50): 13802-13812.

Mori, K., H. Nagao, et al. (1999). "The olfactory bulb: coding and processing of odor molecule information." Science **286**(5440): 711-715.

Muller, D., R. Abel, et al. (2002). "Differential parallel processing of olfactory information in the honeybee, Apis mellifera L." J Comp Physiol A Neuroethol Sens Neural Behav Physiol **188**(5): 359-370.

Ochieng, S. A., K. C. Park, et al. (2002). "Host plant volatiles synergize responses of sex pheromone-specific olfactory receptor neurons in male Helicoverpa zea." J Comp Physiol A Neuroethol Sens Neural Behav Physiol **188**(4): 325-333.

Okada, R., J. Rybak, et al. (2007). "Learning-related plasticity in PE1 and other mushroom body-extrinsic neurons in the honeybee brain." J Neurosci **27**(43): 11736-11747.

Ostojic, S. (2011). "Inter-spike interval distributions of spiking neurons driven by fluctuating inputs." Journal of neurophysiology.

Ro, H., D. Muller, et al. (2007). "Anatomical organization of antennal lobe projection neurons in the moth Heliothis virescens." J Comp Neurol **500**(4): 658-675.

Rostelien, T., A. K. Borg-Karlson, et al. (2000). "Selective receptor neurone responses to E-beta-ocimene, beta-myrcene, E,E-alpha-farnesene and homo-farnesene in the moth Heliothis virescens, identified by gas chromatography linked to electrophysiology." J Comp Physiol A **186**(9): 833-847.

Rostelien, T., M. Stranden, et al. (2005). "Olfactory receptor neurons in two Heliothine moth species responding selectively to aliphatic green leaf volatiles, aromatic compounds, monoterpenes and sesquiterpenes of plant origin." Chem Senses **30**(5): 443-461.

Rubin, B. D. and L. C. Katz (1999). "Optical imaging of odorant representations in the mammalian olfactory bulb." Neuron **23**(3): 499-511.

Ruta, V., S. R. Datta, et al. (2010). "A dimorphic pheromone circuit in Drosophila from sensory input to descending output." Nature **468**(7324): 686-690.

Sachse, S., A. Rappert, et al. (1999). "The spatial representation of chemical structures in the antennal lobe of honeybees: steps towards the olfactory code." Eur J Neurosci **11**(11): 3970-3982.

Sachse, S. and C. G. Galizia (2002). "Role of inhibition for temporal and spatial odor representation in olfactory output neurons: a calcium imaging study." J Neurophysiol **87**(2): 1106-1117.

Sato, K., M. Pellegrino, et al. (2008). "Insect olfactory receptors are heteromeric ligand-gated ion channels." Nature **452**(7190): 1002-1006.

Shepherd, G. M. (1985). "The olfactory system: the uses of neural space for a non-spatial modality." Prog Clin Biol Res **176**: 99-114.

Shinomoto, S., Y. Miyazaki, et al. (2005). "Regional and laminar differences in in vivo firing patterns of primate cortical neurons." Journal of neurophysiology **94**(1): 567-575.

Shinomoto, S., H. Kim, et al. (2009). "Relating neuronal firing patterns to functional differentiation of cerebral cortex." PLoS computational biology **5**(7): e1000433.

Silbering, A. F. and C. G. Galizia (2007). "Processing of odor mixtures in the Drosophila antennal lobe reveals both global inhibition and glomerulus-specific interactions." J Neurosci **27**(44): 11966-11977.

Skiri, H. T., C. G. Galizia, et al. (2004). "Representation of primary plant odorants in the antennal lobe of the moth Heliothis virescens using calcium imaging." Chem Senses **29**(3): 253-267.

Skiri, H. T., H. Ro, et al. (2005). "Consistent organization of glomeruli in the antennal lobes of related species of heliothine moths." J Comp Neurol **491**(4): 367-380.

Smith, G. D., C. L. Cox, et al. (2000). "Fourier analysis of sinusoidally driven thalamocortical relay neurons and a minimal integrate-and-fire-or-burst model." Journal of neurophysiology **83**(1): 588-610.

Strausfeld, N. J. and J. G. Hildebrand (1999). "Olfactory systems: common design, uncommon origins?" Current Opinion in Neurobiology **9**(5): 634-639.

Sun, X. J., C. Fonta, et al. (1993). "Odor Quality Processing by Bee Antennal Lobe Interneurons." Chemical Senses **18**(4): 355-377.

Vickers, N. J. (2006). "Winging it: moth flight behavior and responses of olfactory neurons are shaped by pheromone plume dynamics." Chem Senses **31**(2): 155-166.

Vosshall, L. B. and R. F. Stocker (2007). "Molecular architecture of smell and taste in Drosophila." Annu Rev Neurosci **30**: 505-533.

Yarmolinsky, D. A., C. S. Zuker, et al. (2009). "Common Sense about Taste: From Mammals to Insects." Cell **139**(2): 234-244.

APPENDIX I: Cluster analysis

Distance Algorithms

(adapted from www.MathWorks.com)

ISI distribution data was presented as an *m-by-n* (39 neurons x 60 ISI bins) data matrix *X*, which was treated as *m (1-by-n)* row vectors $x_1, x_2, \ldots, x_m$, the various distances between the vector x_s and x_t were defined as follows:

Euclidean distance:

$$d_{st}^2 = \sum_{i=1}^{60} (x_{s,i} - x_{t,i})^2$$

Standardized Euclidean distance:

$$d_{st}^2 = \sum_{i=1}^{60} (x_{s,i} - x_{t,i})^2 V^{-1}$$

where *V* is the *n-by-n* diagonal matrix whose *j'*th diagonal element is $S(j)^2$, where *S* is the vector of standard deviations

Cityblock distance:

$$d_{st} = \sum_{i=1}^{60} |x_{s,i} - x_{t,i}|$$

Cosine distance:

$$d_{st} = 1 - \frac{\sum_{i=1}^{60} x_{s,i} x_{t,i}}{\sqrt{\sum_{i=1}^{60} x_{s,i}^2} \sqrt{\sum_{i=1}^{60} x_{t,i}^2}}$$

Correlation distance:

$$d_{st} = 1 - \frac{\sum_{i=1}^{60} (x_{s,i} - \overline{x_s})(x_{t,i} - \overline{x_t})}{\sqrt{\sum_{i=1}^{60} (x_{s,i} - \overline{x_s})^2} \sqrt{\sum_{i=1}^{60} (x_{t,i} - \overline{x_t})^2}},$$

where $\overline{x_s} = \frac{1}{60} \sum_i x_{s,i}$ and $\overline{x_t} = \frac{1}{60} \sum_i x_{t,i}$

Linkage algorithms

(adapted from www.MathWorks.com)

The following notation is used to describe the linkages used by the various methods:

- Cluster r is formed from clusters p and q
- n_r is the number of objects in cluster r
- x_{ri} is the i'th object in cluster r

Average linkage uses the average distance between all pairs of objects in any two clusters:

$$d(r,s)=\frac{1}{n_r n_s}\sum_{i=1}^{n_r}\sum_{j=1}^{n_s}(x_{ri},x_{sj})$$

Centroid linkage uses the Euclidean distance between the centroids of the two clusters:

$d(r,s)=\|\overline{x_r}-\overline{x_s}\|_2$, where $\overline{x_r}=\frac{1}{n_r}\sum_{i=1}^{n_r}x_{ri}$ and $\|\ \|_2$ is Euclidean distance

Ward's linkage uses the incremental sum of squares; that is, the increase in the total within-cluster sum of squares as a result of joining two clusters. The within-cluster sum of squares is defined as the sum of the squares of the distances between all objects in the cluster and the centroid of the cluster. The sum of squares measure is equivalent to the following distance measure $d(r,s)$, which is the formula `linkage` uses:

$$d(r,s)=\sqrt{\frac{2\mathrm{n}_r n_s}{n_r+n_s}\|\overline{x_r}-\overline{x_s}\|_2^2}$$, where:

- $\|\ \|_2$ is Euclidean distance
- $\overline{x_r}$ and $\overline{x_s}$ are the centroids of clusters r and s
- n_r and n_s are the number of elements in clusters r and s

Weighted average linkage uses a recursive definition for the distance between two clusters. If cluster r was created by combining clusters p and q, the distance between r and another cluster s is defined as the average of the distance between p and s and the distance between q and s:

$$d(r,s)=\frac{(d(p,s)+d(q,s))}{2}$$

Cluster dendrograms

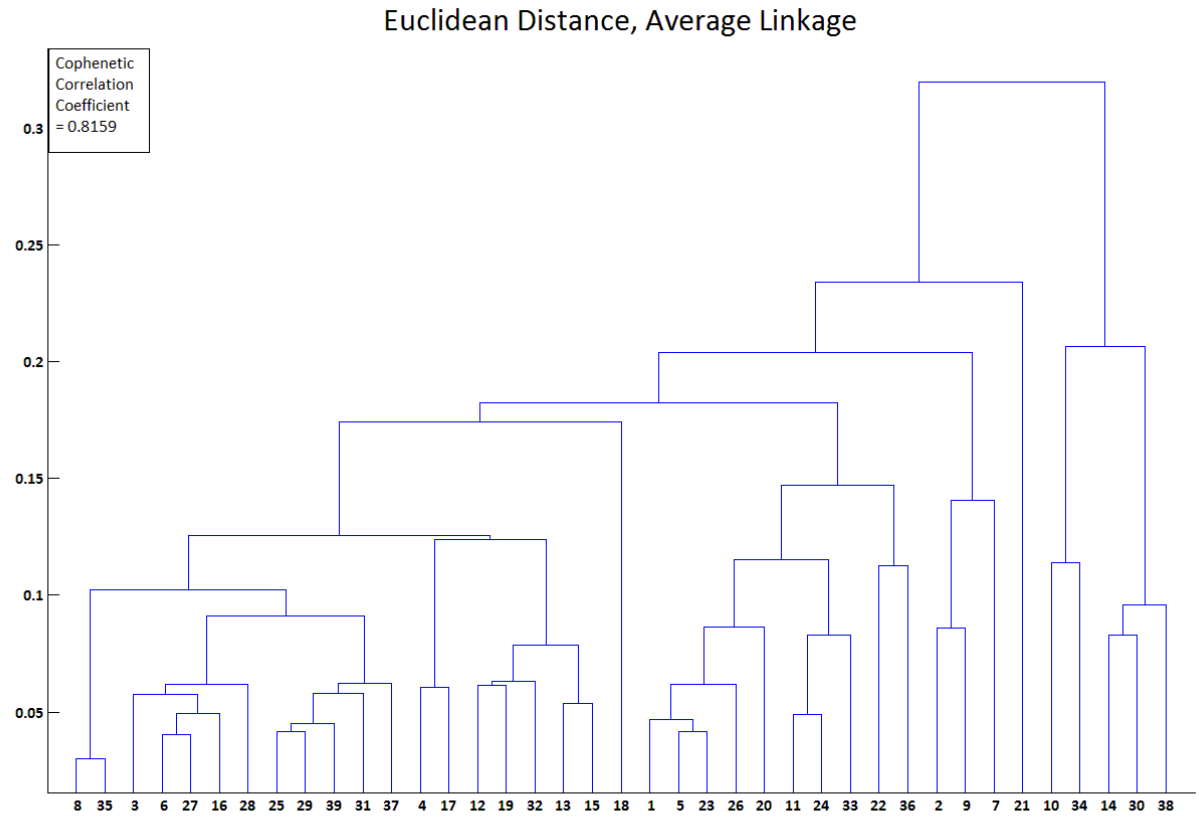

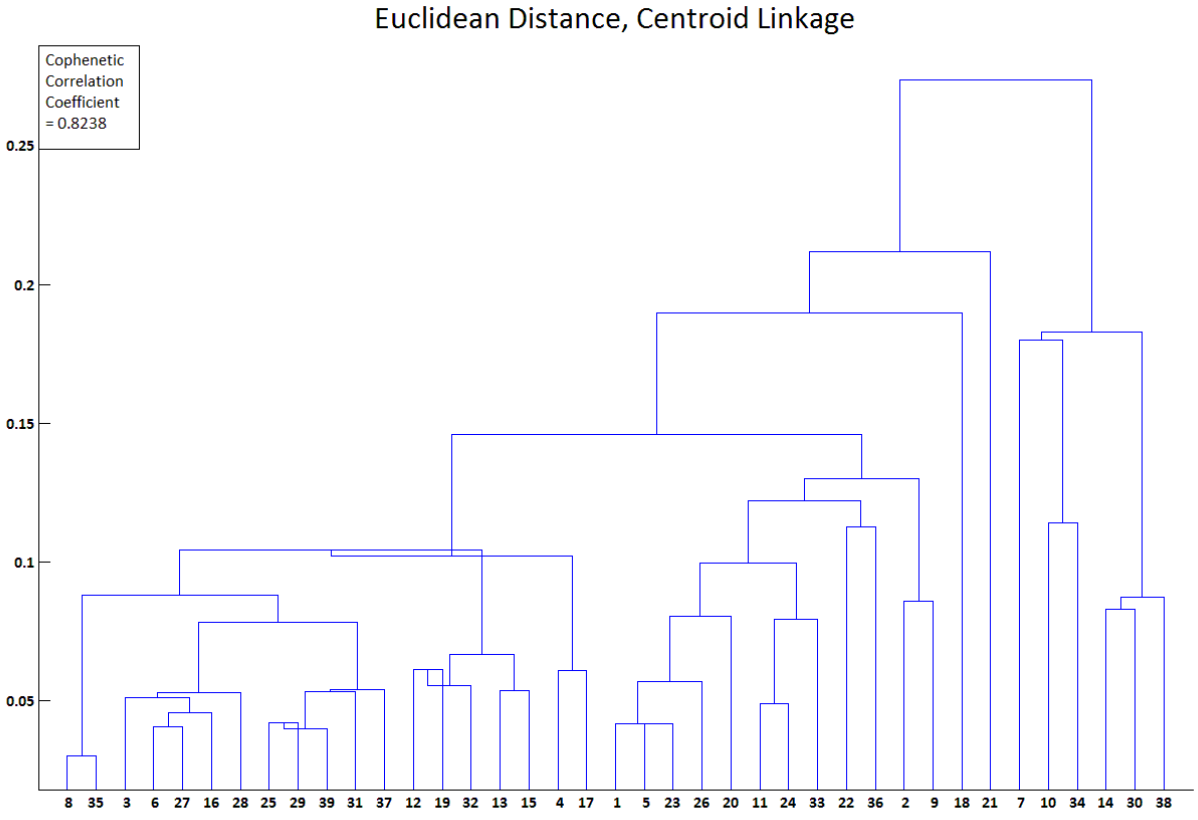

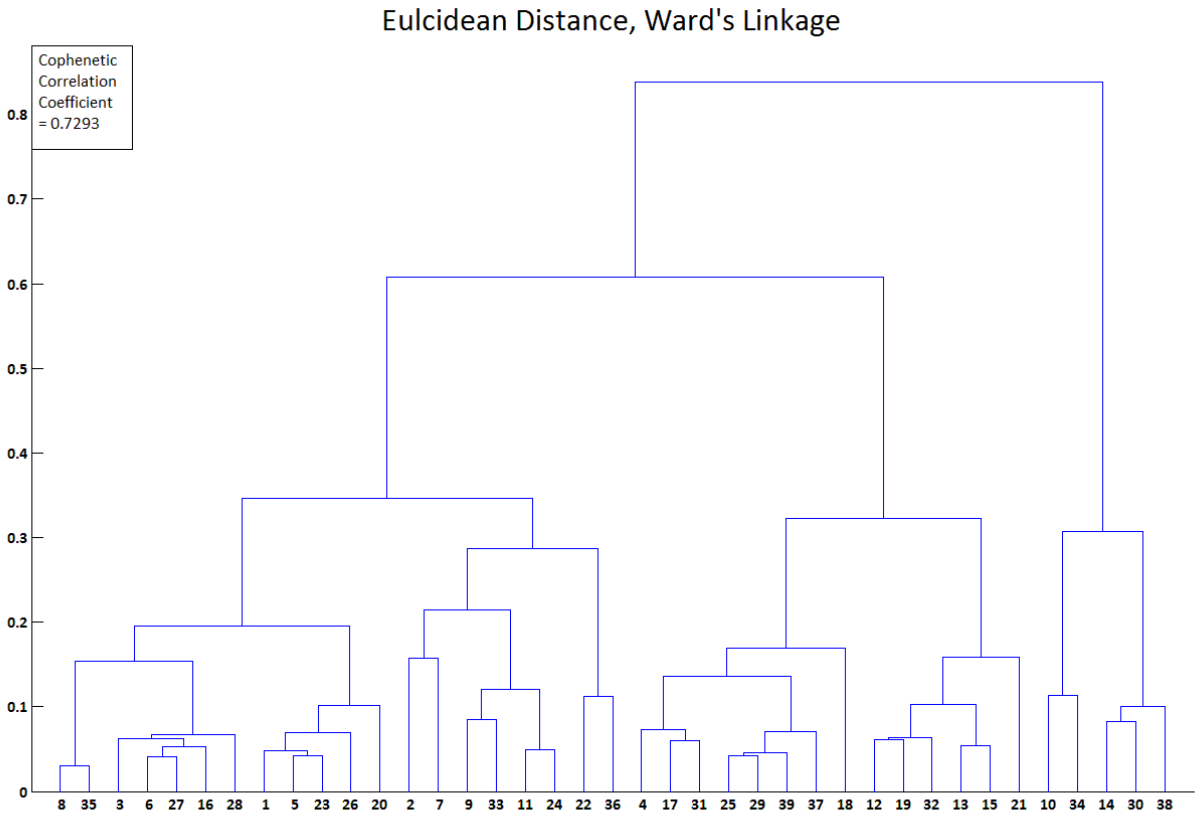
Eulcidean Distance, Ward's Linkage
Cophenetic Correlation Coefficient = 0.7293
0.8
0.7
0.6
0.5
0.4
0.3
0.2
0.1
0
8 35 3 6 27 16 28 1 5 23 26 20 2 7 9 33 11 24 22 36 4 17 31 25 29 39 37 18 12 19 32 13 15 21 10 34 14 30 38

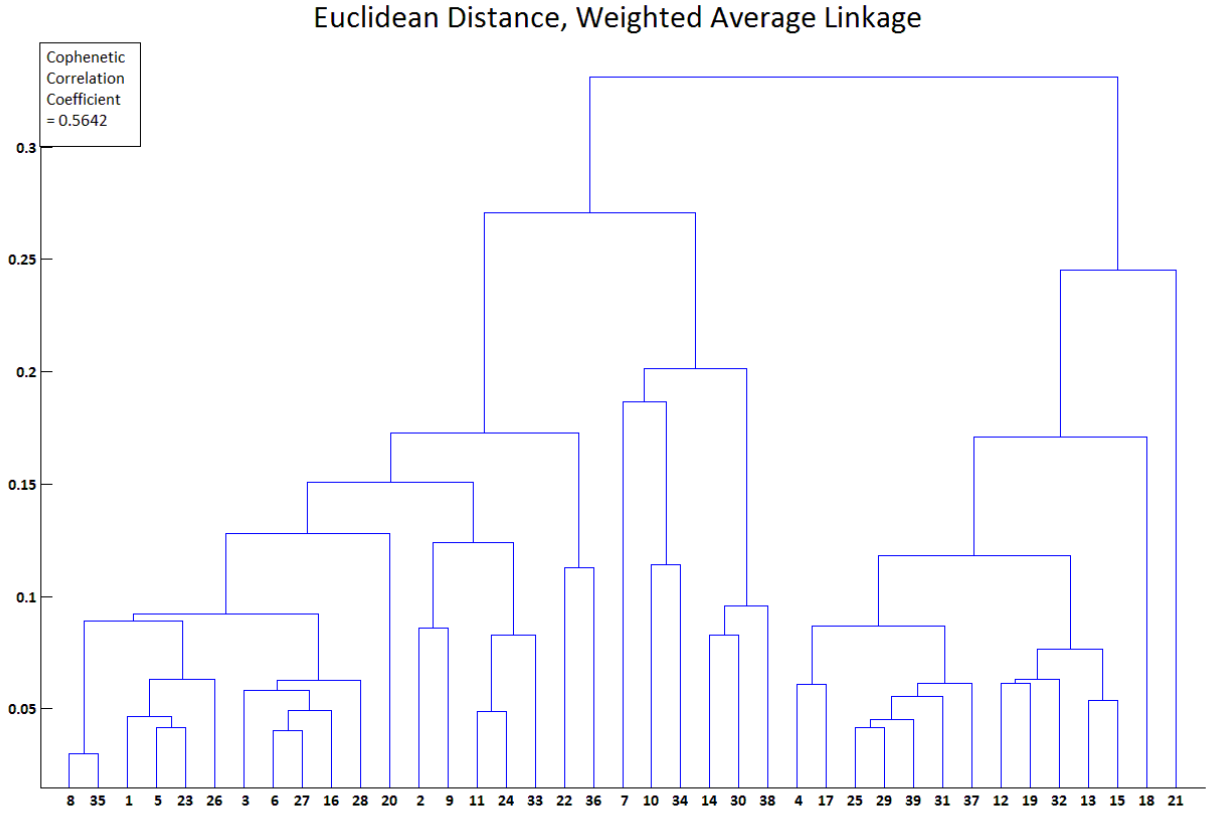
Euclidean Distance, Weighted Average Linkage
Cophenetic Correlation Coefficient = 0.5642
0.3
0.25
0.2
0.15
0.1
0.05
8 35 1 5 23 26 3 6 27 16 28 20 2 9 11 24 33 22 36 7 10 34 14 30 38 4 17 25 29 39 31 37 12 19 32 13 15 18 21

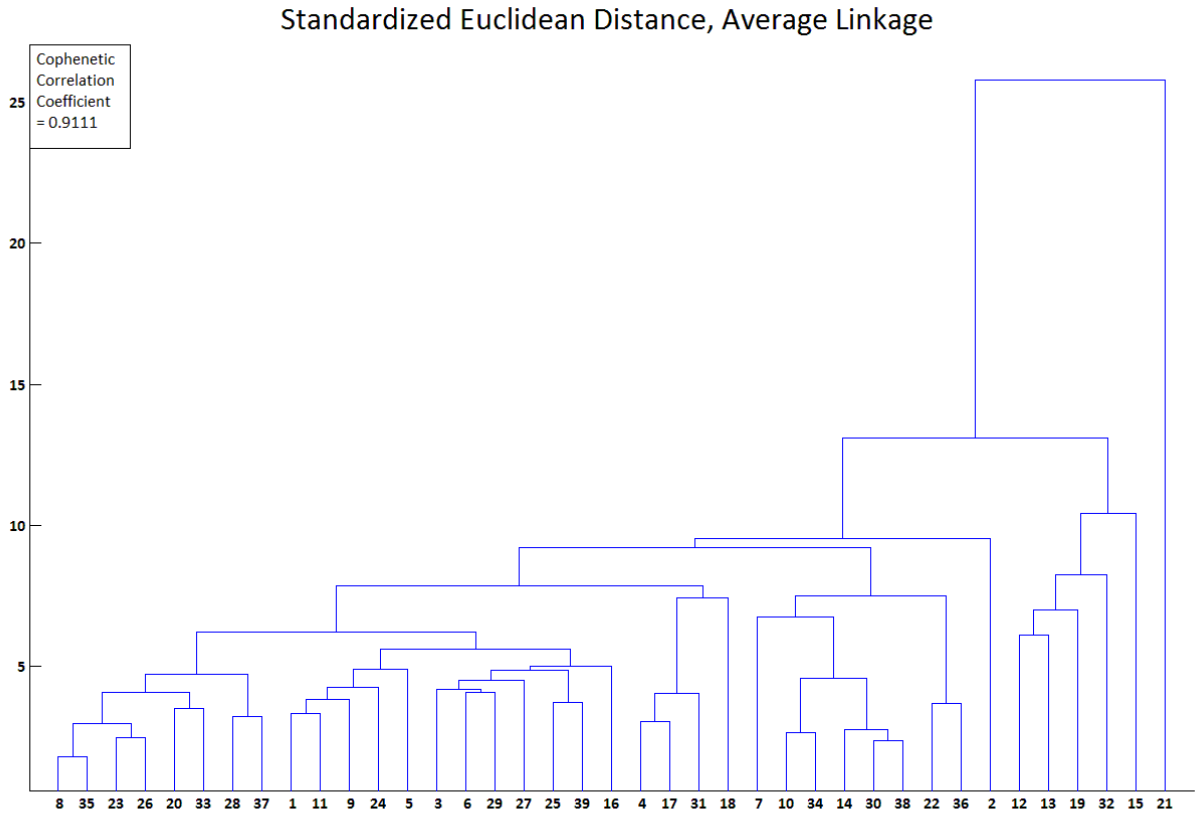
Standardized Euclidean Distance, Average Linkage
Cophenetic Correlation Coefficient = 0.9111
25
20
15
10
5
8 35 23 26 20 33 28 37 1 11 9 24 5 3 6 29 27 25 39 16 4 17 31 18 7 10 34 14 30 38 22 36 2 12 13 19 32 15 21

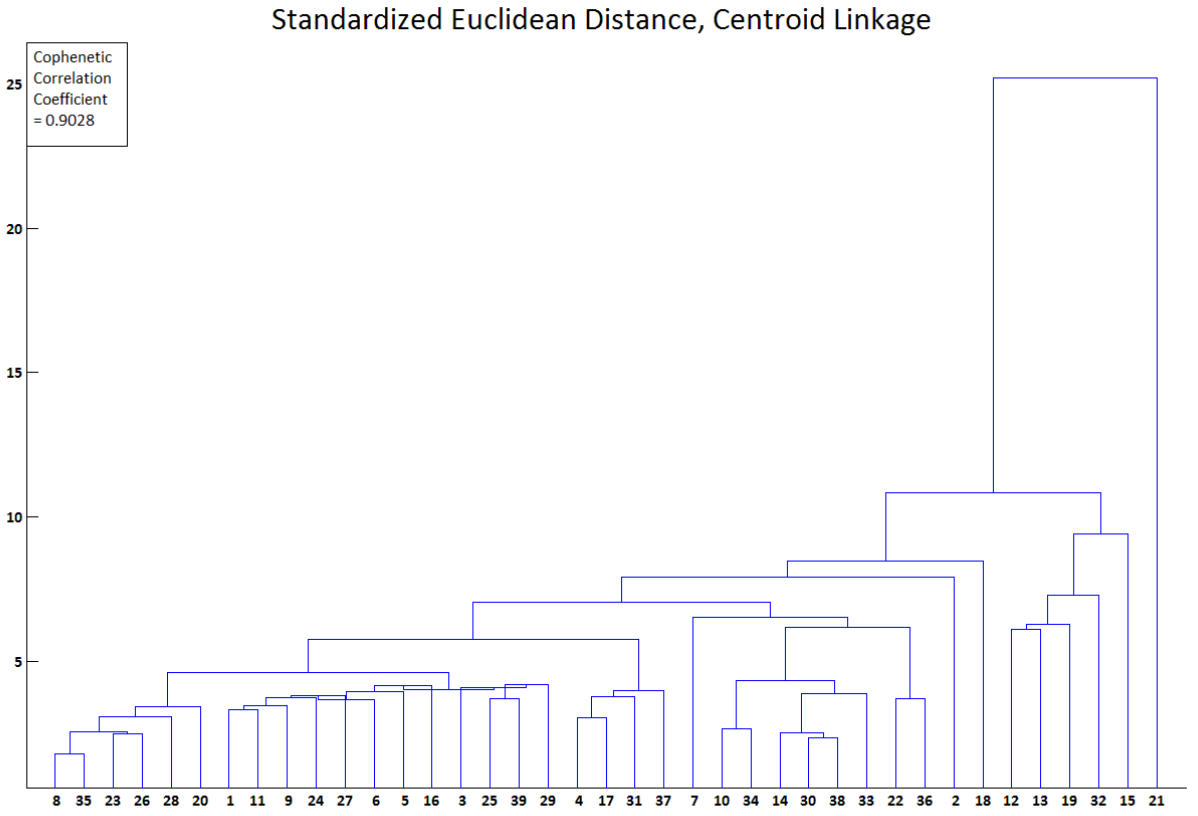
Standardized Euclidean Distance, Centroid Linkage
Cophenetic Correlation Coefficient = 0.9028
25
20
15
10
5
8 35 23 26 28 20 1 11 9 24 27 6 5 16 3 25 39 29 4 17 31 37 7 10 34 14 30 38 33 22 36 2 18 12 13 19 32 15 21

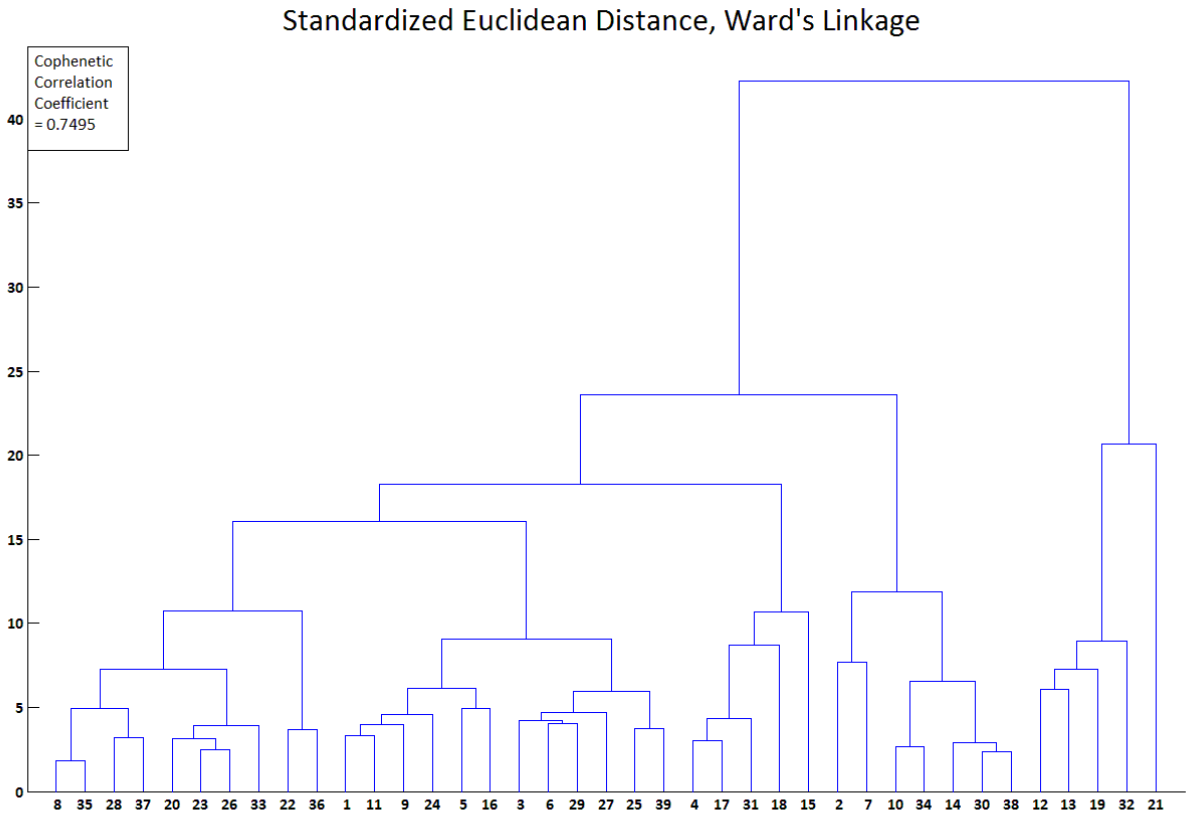
Standardized Euclidean Distance, Ward's Linkage
Cophenetic Correlation Coefficient = 0.7495
0 5 10 15 20 25 30 35 40
8 35 28 37 20 23 26 33 22 36 1 11 9 24 5 16 3 6 29 27 25 39 4 17 31 18 15 2 7 10 34 14 30 38 12 13 19 32 21

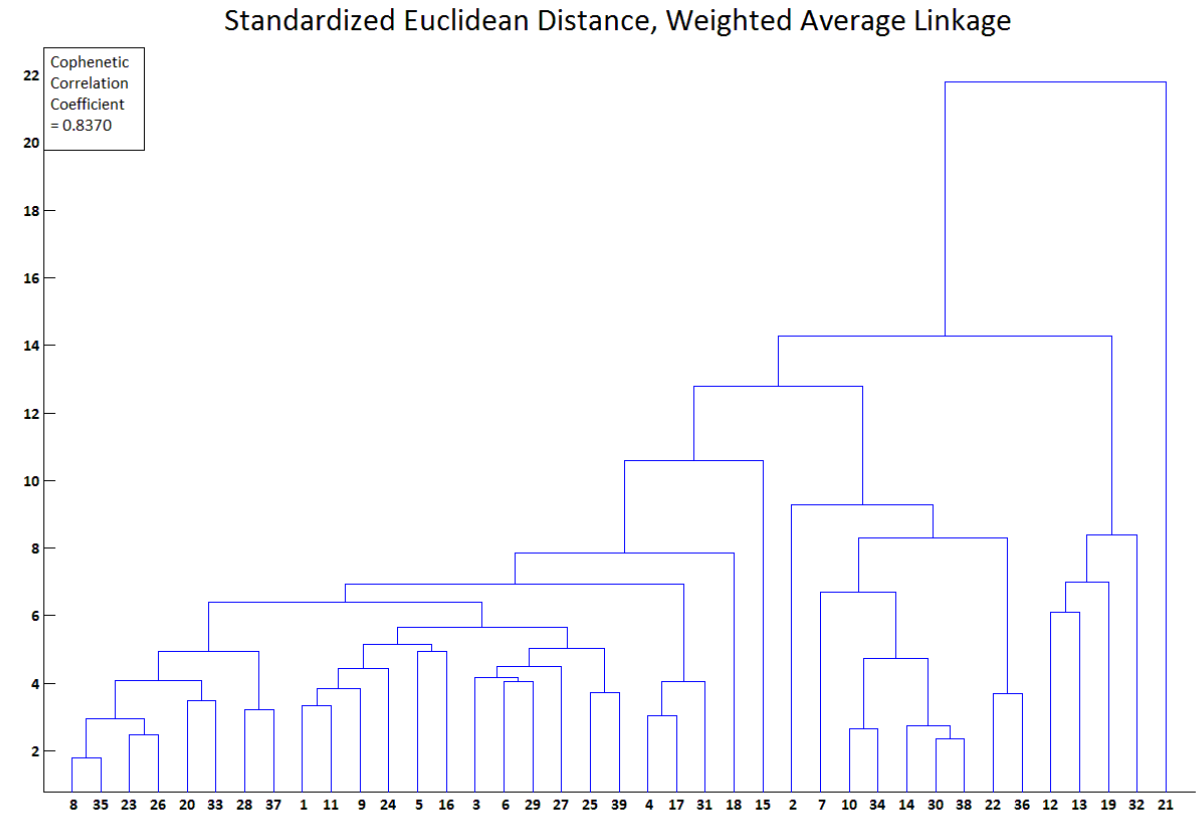
Standardized Euclidean Distance, Weighted Average Linkage
Cophenetic Correlation Coefficient = 0.8370
2 4 6 8 10 12 14 16 18 20 22
8 35 23 26 20 33 28 37 1 11 9 24 5 16 3 6 29 27 25 39 4 17 31 18 15 2 7 10 34 14 30 38 22 36 12 13 19 32 21

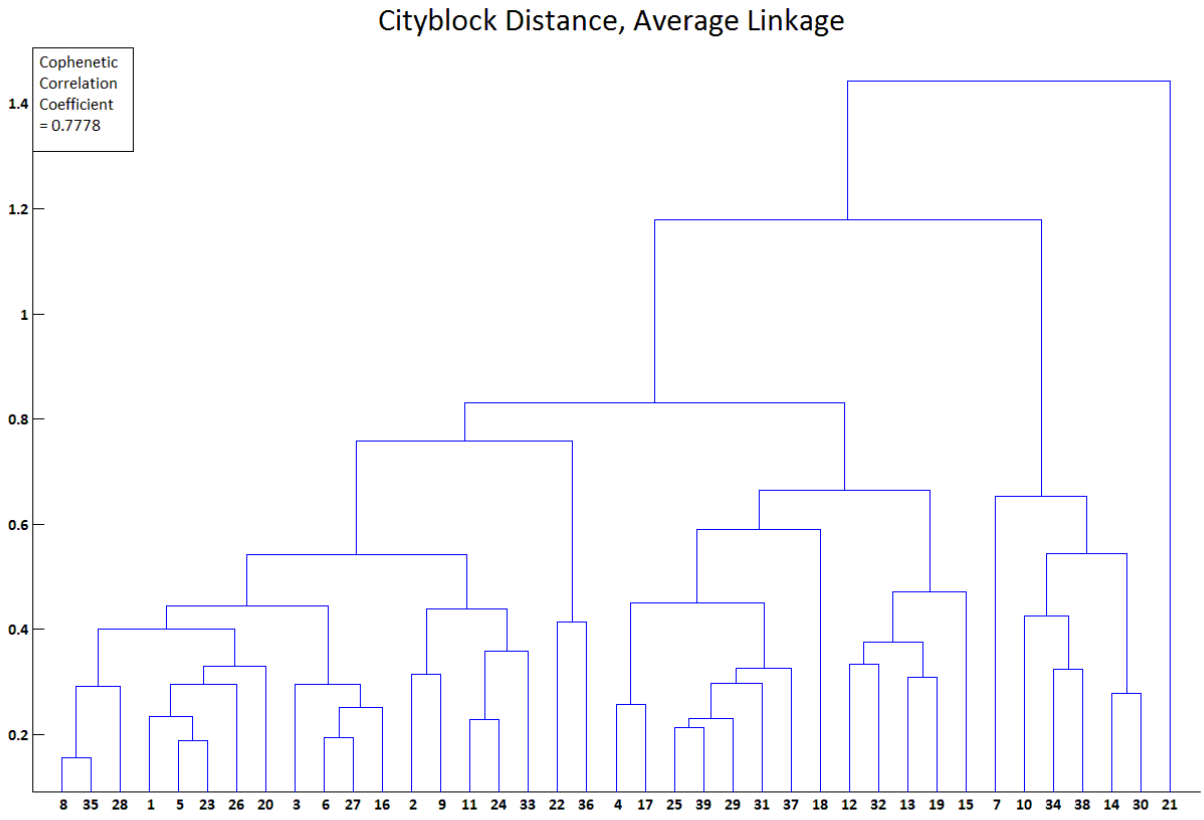
Cityblock Distance, Average Linkage
Cophenetic Correlation Coefficient = 0.7778
1.4
1.2
1
0.8
0.6
0.4
0.2
8 35 28 1 5 23 26 20 3 6 27 16 2 9 11 24 33 22 36 4 17 25 39 29 31 37 18 12 32 13 19 15 7 10 34 38 14 30 21

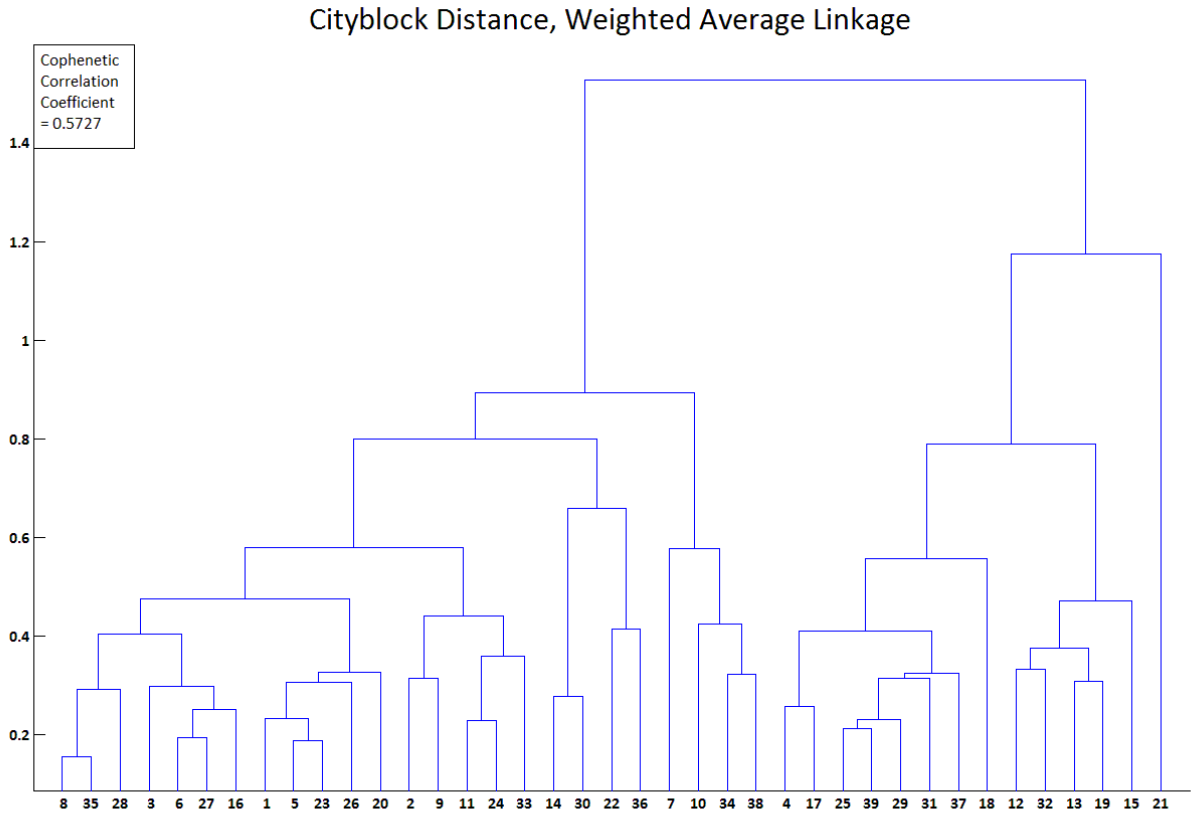
Cityblock Distance, Weighted Average Linkage
Cophenetic Correlation Coefficient = 0.5727
1.4
1.2
1
0.8
0.6
0.4
0.2
8 35 28 3 6 27 16 1 5 23 26 20 2 9 11 24 33 14 30 22 36 7 10 34 38 4 17 25 39 29 31 37 18 12 32 13 19 15 21

Correlation Distance, Weigthed Average Linkage

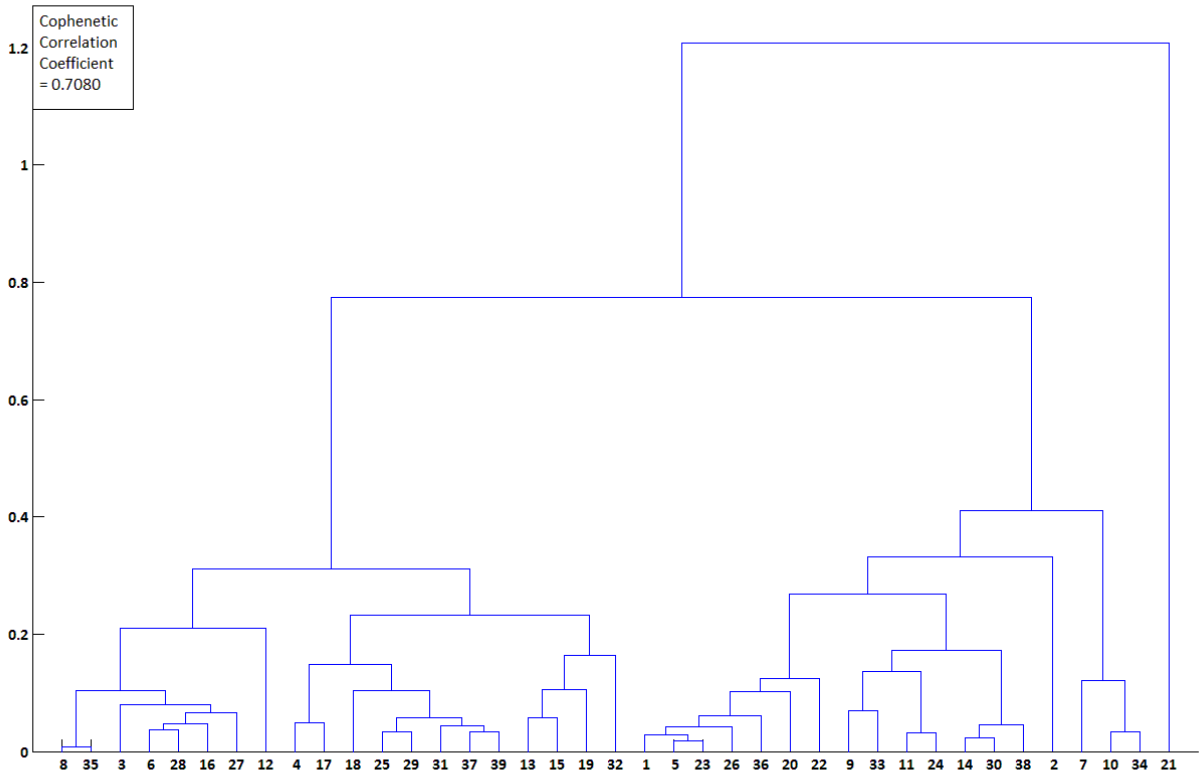

Correlation Distance, Average Linkage

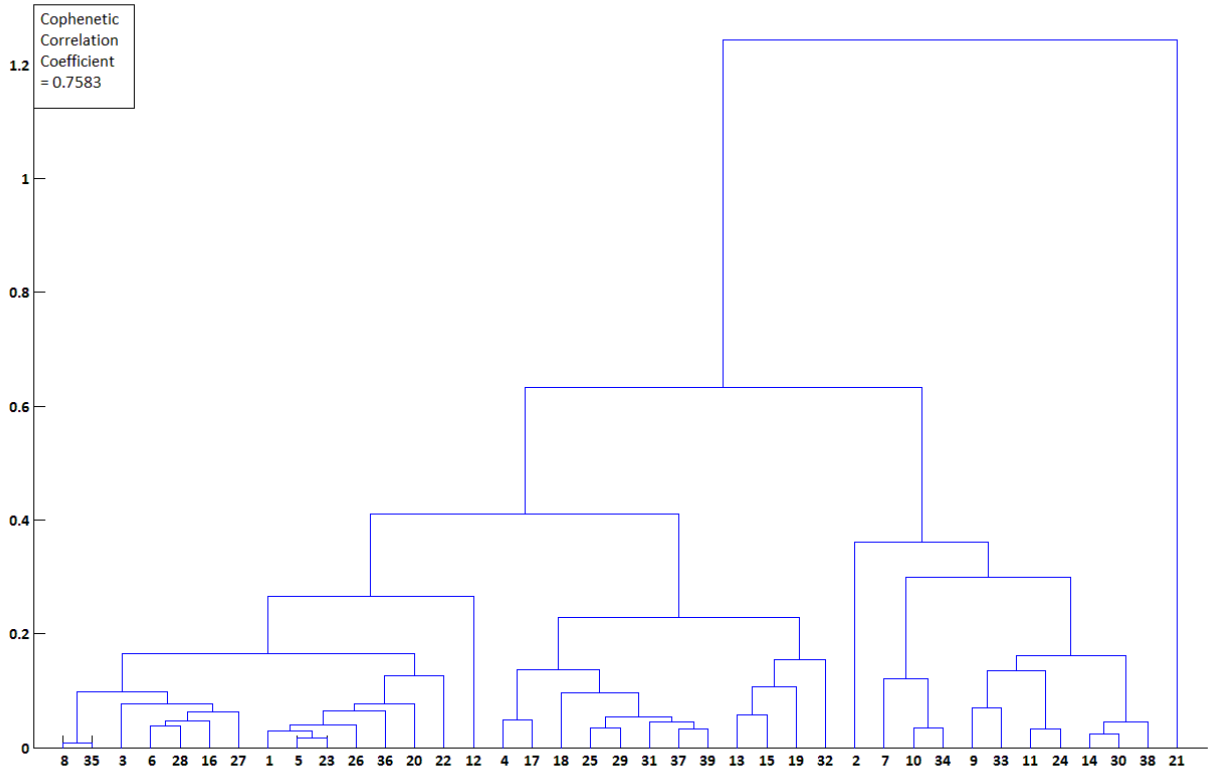

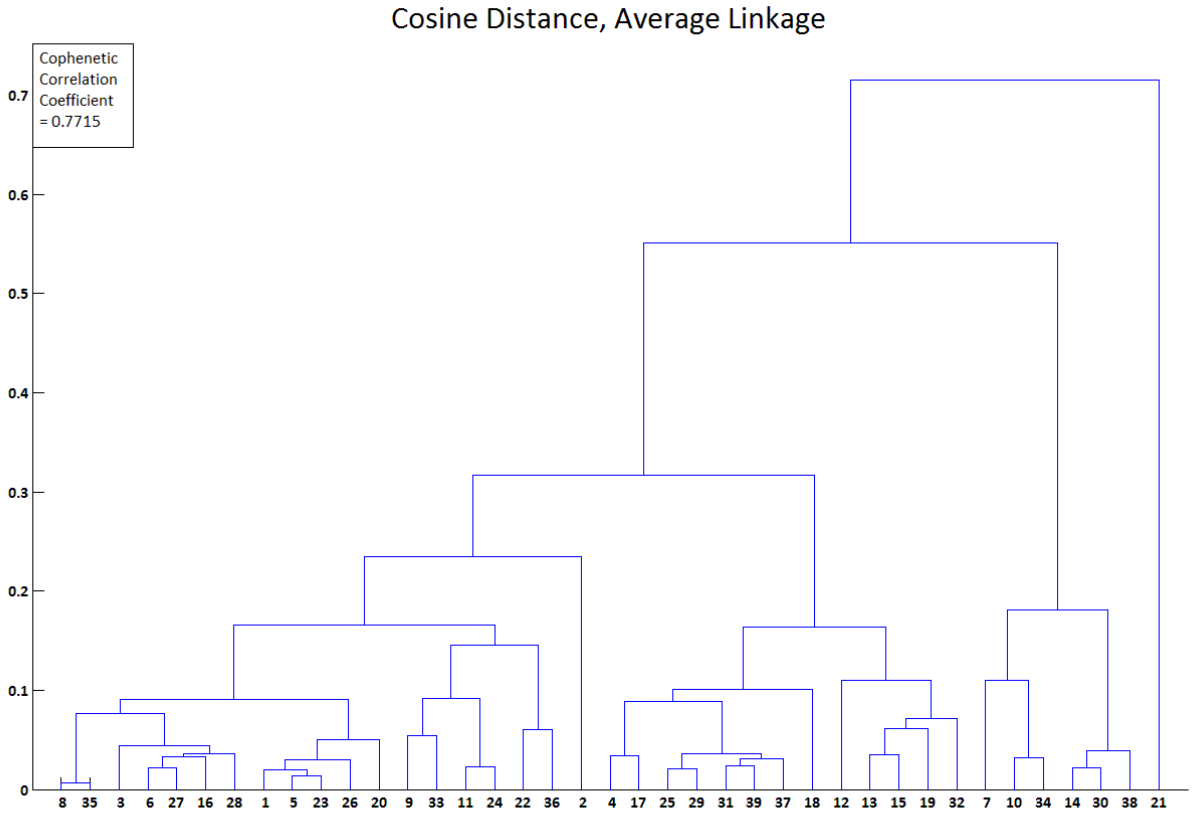
Cosine Distance, Average Linkage
Cophenetic Correlation Coefficient = 0.7715
0.7
0.6
0.5
0.4
0.3
0.2
0.1
0
8 35 3 6 27 16 28 1 5 23 26 20 9 33 11 24 22 36 2 4 17 25 29 31 39 37 18 12 13 15 19 32 7 10 34 14 30 38 21

APPENDIX II

Blend Composition

Table 4: Composition of the 6 blends used. Shaded field means included, open field means excluded.

Single Components	Blends					
	B1	**B2**	**B9**	**B10**	**B11**	**B12**
3Z-hexenol						
3Z-hexenyl acetate						
ocimene						
linalool						
geraniol						
3-carene						
E-verbenol						
methyl benzoate						
hexanol						
phenylethanol						
farnesenes						
germacrene -D						

PSTH examples from three protocerebral neurons

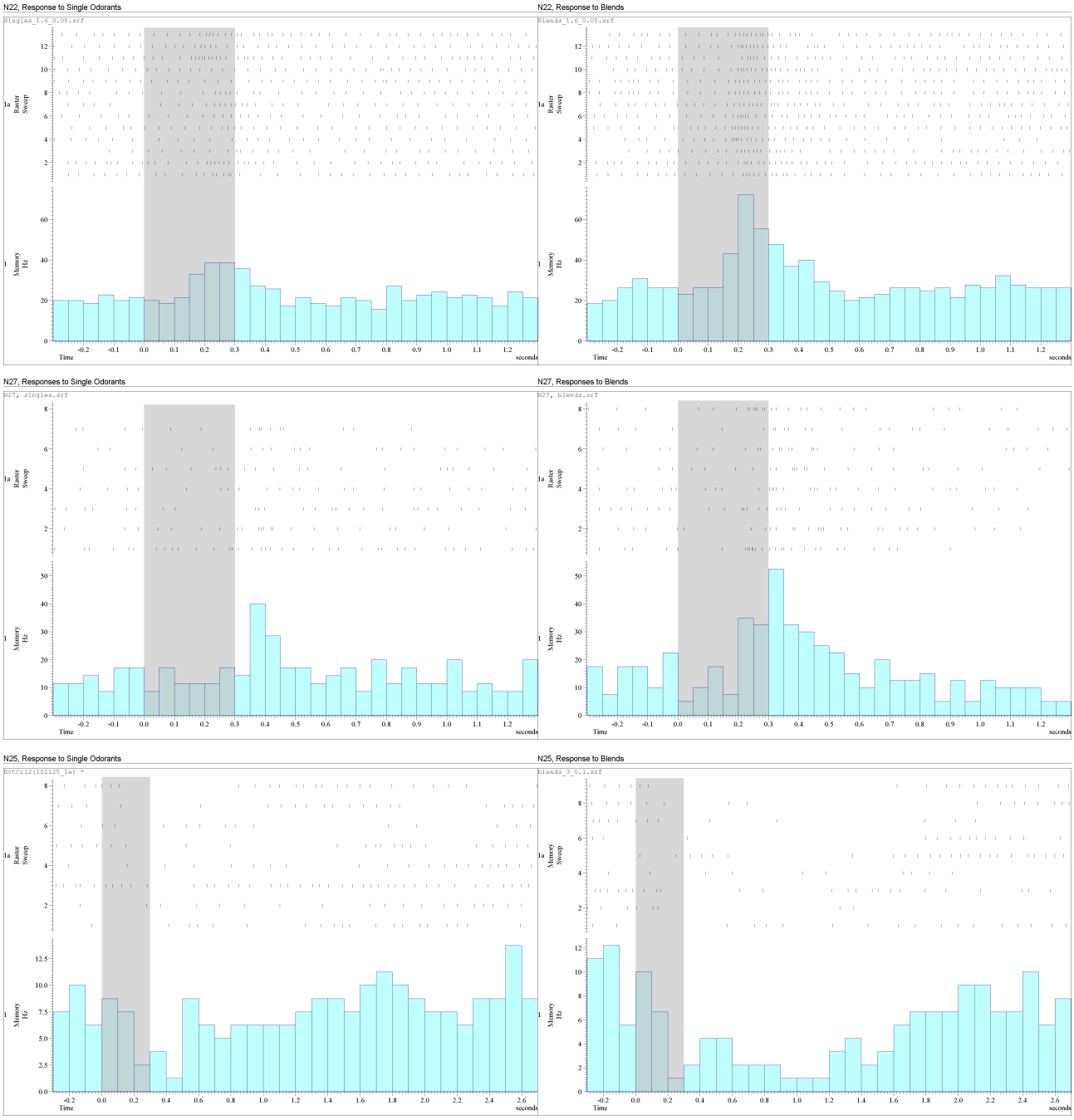

Figure 11: Raster plots and PSTH of 3 of the protocerebral neurons (N22, N25, N27) that were selected for both the TRS comparison analysis and the ISI cluster analysis. All three neurons showed significantly stronger TRS to blends (right column) than single odorants (left column) (α = 0.05). N22 (top) and N27 (middle) responded typically with excitation, whereas N25 (bottom) reponded with inhibition to bot single odorants and blends. N25 and N27 had quite similar ISI distributions, even though they responded differently. Both these neurons had quite unstable spontaneous activity.

N40, MB extrinsic neuron

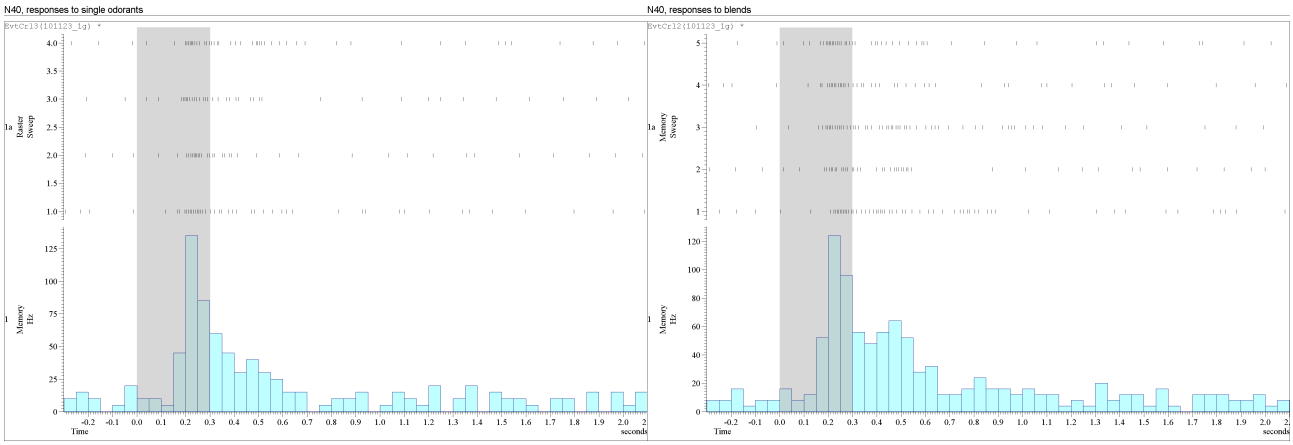

Figure 12: PSTH of single odorants (left) and blends (right). Maximum firing rate is found in the range of 250-300 ms post stimulus onset, measuring approximately ~130 Hz for single odorant, and ~125 Hz for blends (not significantly different). However, the blends have a longer lasting excitation, and TRS is found to be significantly different (α = 0.05) between singles and blends. Notice the bimodal response is also clearer for the blends. Doublets and triplets of spikes were observed several places in the recording.

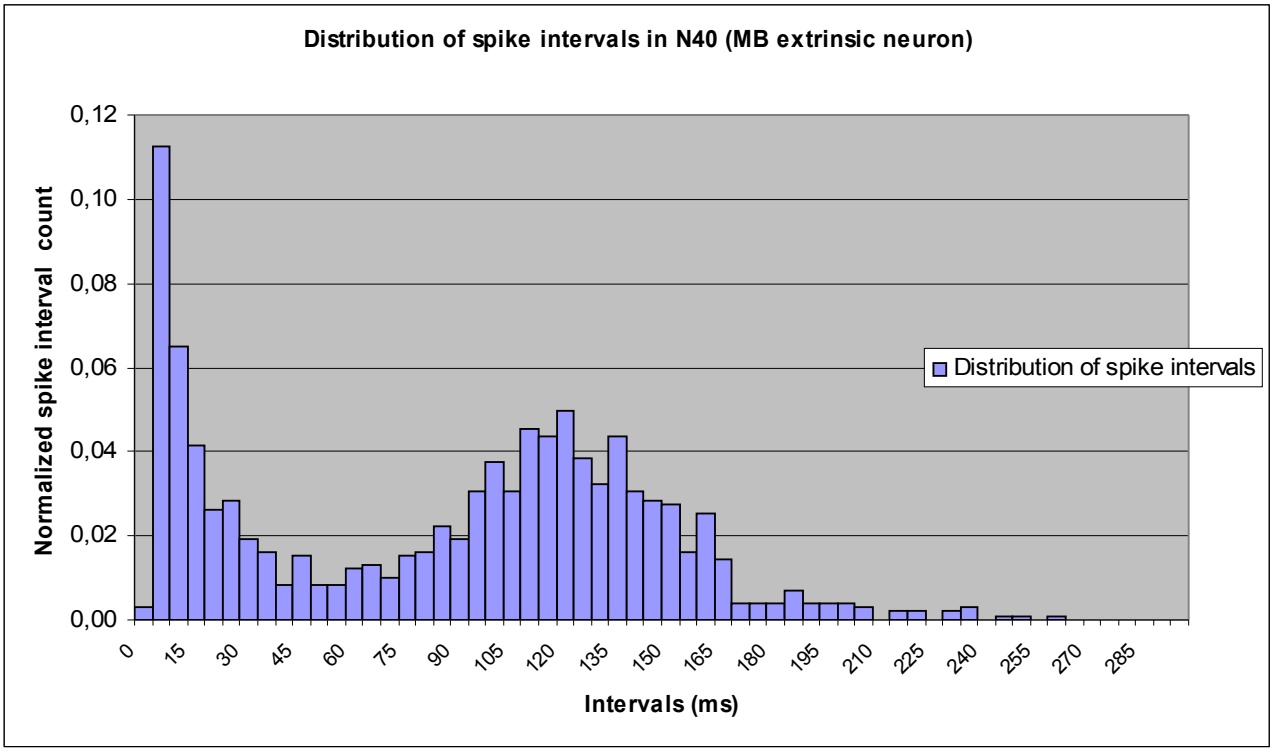

Figure 13: Estimated ISI distribution of MB extrinsic neuron N40, showing a clear bimodal shape. Total number of ISIs were 987, which is less than the criterion limit set for the cluster analysis (>1500). Thefirst peak of 10-20ms intervals, is constituted by the responses to odorants. Significantly stronger responses to blends than to single odorants were found (figure 8).